Ore Geology Reviews 101 (2018) 312–329

Contents lists available at ScienceDirect

Ore Geology Reviews

journal homepage: www.elsevier.com/locate/oregeorev

Petrology, geochemistry and stable isotope studies of the Miocene igneous rocks and related sulphide mineralisation of Oued Amizour (NE Algeria)

Rabah Laouar[a,e,*], Abdelmalek Lekoui[b], Tayeb Bouima[c], Sihem Salmi-Laouar[a], Salah Bouhlel[d], Nachida Abdallah[e], Adrian J. Boyce[f], Anthony E. Fallick[f]

[a] Département de Géologie, Faculté des Sciences de la Terre, Université Badji-Mokhtar Annaba, B.P. 12, 23000 Annaba, Algeria
[b] Département des Sciences de la Terre et de l'Univers, Université Mohamed Seddik Ben Yahia, 18000 Jijel, Laboratoire de génie géologique Jijel, Algeria
[c] Institut d'Architecture et des Sciences de la Terre, Université Farhat Abbas Sétif, 19000 Sétif, Algeria
[d] Mineral Resources Team, LRM2E, Geology Department, Faculty of Sciences, University Tunis El Manar, Tunis 2092, Tunisia
[e] Laboratoire de Géodynamique, Géologie de l'Ingénieur et Planétologie, F.S.T.G.A.T., USTHB, BP. 32, Bab Ezzouar, 16111 Algiers, Algeria
[f] Isotope Geosciences Unit, S.U.E.R.C., East Kilbride, Glasgow G75 0QU, Scotland, UK

ARTICLE INFO

Keywords:
Igneous rocks
Calc-alkaline
Zn-deposit
Hydrothermal alteration
Stable isotopes
Oued Amizour

ABSTRACT

The Oued Amizour granitoids of North Africa were studied in order to assess the role of magma processes in the formation of the large Zn-deposit in the region. Access to material from a ~800 m drillhole cutting the entire igneous succession greatly facilitated the investigation. The rocks reveal, from the top to the bottom, two distinct lithologies: volcanic, mainly pyroclastic rocks and sub-volcanic microgranitic – plutonic granodioritic rocks. Both lithologies were subject to hydrothermal alteration. The boundary between the two lithologies is marked by a massive, ~10 m thick anhydrite layer. The geochemistry of these rocks shows that they are intermediate to felsic in composition and exhibit high-K to shoshonitic calc-alkaline features with I-type signature. The negative Eu, Sr and Nb anomalies and the high LILE and LREE enrichment observed in the whole igneous suite indicate that the various volcanic and plutonic rocks are genetically related. The granitoids are considered to have formed under post-collisional geotectonic regime during the Miocene, similar to those described in the Alpine Belt of northern Africa.

The main sulphide mineralisation is dominated by sphalerite with rare marcasite, melnikovite, galena and minor but ubiquitous pyrite. The sphalerite ore body of about 20–30 m thick is hosted by hydrothermally altered andesite breccias and volcanic tuff, between the anhydrite layer at the base and the volcanic pile at the top. Replacement, colloform and open space filling are the main ore texture patterns which indicate hydrothermal processes throughout successive percolation phases.

$\delta^{34}S$ of sulphides (sphalerite, pyrite and chalcopyrite) vary between −7.2‰ and +4.5‰ (n = 22; mean = −1.3‰), suggesting that magmatic fluids have played a major role in the formation of the Oued Amizour Zn-deposit. However, $\delta^{34}S$ of sulphates (anhydrite and gypsum) which are isotopically heavier ranging between +13.2‰ and +20.6‰ (n = 10; mean = +16.3‰), likely reflect mixing between Miocene seawater sulphate and magmatic sulphur. Fluid inclusion microthermometric measurements on anhydrite and gangue calcite yield a mean temperature of ~200 °C and salinity between 22.3 and 26.6% eq. NaCl. Calcite $\delta^{18}O_{V\text{-}SMOW}$ varies between +11.2 and +20.2‰ (n = 12, mean = +16.7‰) and $\delta^{13}C_{V\text{-}PDB}$ varies between −3.7 and −11.0‰ (mean = −7.8‰). These results confirm the magmatic origin of the mineralising fluids, with a marked contribution of seawater, for precipitation of the Oued Amizour Zn mineralisation. Low $\delta^{13}C_{V\text{-}PDB}$ could, however, be attributed to the contribution of carbon from unconsolidated mudstones and/or magmatic carbon. The observed data on the Oued Amizour Zn deposit show that the mineralisation is part of VHMS group with a Kuroko-type signature.

* Corresponding author at: Département de Géologie, Faculté des Sciences de la Terre, Université Badji-Mokhtar Annaba, B.P. 12, 23000 Annaba, Algeria.
E-mail addresses: rabahlaouar@yahoo.fr (R. Laouar), lekouim@yahoo.fr (A. Lekoui), tbouima@yahoo.fr (T. Bouima), ssalmit@yahoo.fr (S. Salmi-Laouar), salah.bouhlel@fst.rnu.tn (S. Bouhlel), a_nachida@yahoo.fr (N. Abdallah), a.boyce@suerc.gla.ac.uk (A.J. Boyce), Anthony.Fallick@glasgow.ac.uk (A.E. Fallick).

https://doi.org/10.1016/j.oregeorev.2018.07.026
Received 5 November 2017; Received in revised form 25 July 2018; Accepted 27 July 2018
Available online 29 July 2018
0169-1368/

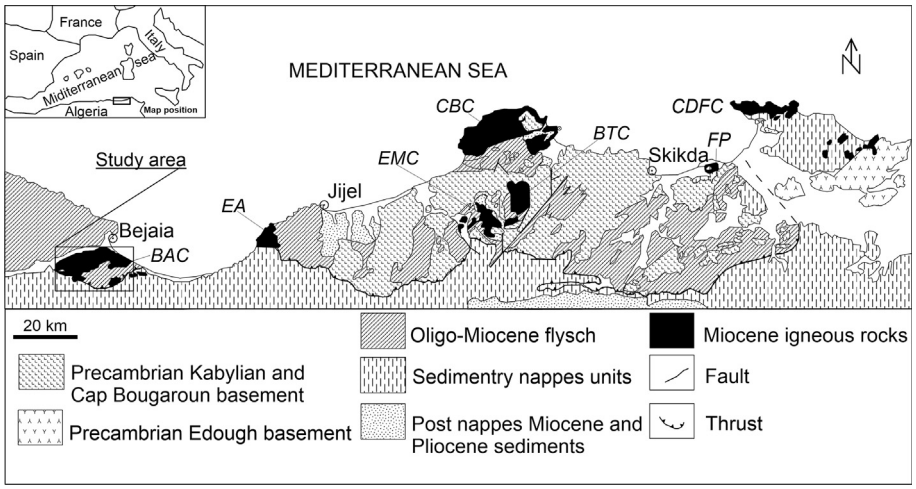

Fig. 1. Geological sketch map of northeastern Algeria showing the location of the igneous complexes. CBC: Cap Bougaroun, BTC: Beni Touffout, EMC: El Milia, FP: Filfila peraluminous plutons, BAC: Bejaia–Amizour, EA: El Aouana, CDFC: Chetaibi-Cap de Fer. (Modified from Durand-Delga, 1978; Vila, 1980; Fourcade et al., 2001).

1. Introduction

A number of Miocene igneous rocks crop out along the North African margin and are distributed from the Galite Isle in Tunisia along the Algerian coast to northern Morocco. The emplacement of these igneous rocks is believed to be a consequence the western Mediterranean subduction-collision between the African and European plates during the Oligo-Miocene (e.g., Auzende et al., 1975; Cohen, 1980; Maury et al., 2000; Carminati et al., 2012; Chazot et al., 2017). This tectonic episode was also responsible for the actual tectonic structure of the so-called Alpine Belt of the western Mediterranean Basin (e.g., Bellon, 1976; Durand-Delga and Fontboté, 1980).

In northern Algeria, the composition of the Miocene magmatic rocks ranges from predominantly mafic compositions in the west to felsic compositions in the east showing different emplacement conditions from plutonic through sub-volcanic to volcanic environments (Benali, 2007). The igneous bodies in northeastern Algeria intruded both the metamorphic basement and the overlying sedimentary cover of the Internal Zones (Fig. 1) at ca. 17–11 Ma (Bellon, 1981; Marignac and Zimmermann, 1983; Abbassene et al., 2016). The previous geological, geochemical and isotopic studies on these rocks (e.g., Hilly, 1962; Fougnot, 1990; Ouabadi et al., 1992, Ouabadi, 1994; Ahmed-Said et al., 1993; Semroud et al., 1994; Laouar et al., 2002; Laouar et al., 2005; Bouabsa et al., 2010; Maury et al., 2000) show two post-collisional main types of magmas: a mantle-derived magma which has undergone variable crustal contamination (e.g., Edough, Chetaibi and Cap de Fer; Laouar et al., 2002; Laouar et al., 2005) and a magma generated by partial melting of metasedimentary rocks (e.g., Cap Bougaroun Filfila; Ouabadi et al., 1992; Bouabsa et al., 2010). The petrological and geochemical features of these two types of magmas correspond to the I-type and S-type granitoid classification of Chappell and White (1974, 2001) respectively.

The magmatic activity in northeastern Algeria was accompanied by various degrees of hydrothermal fluid circulation which resulted in three main types of mineralisation: (1) Pb-Zn-Cu vein ores; (2) W–As–Au deposits related to skarns; and (3) Sb–Au vein mineralisation. These are exposed either as small prospects (e.g., Chetaibi-Cap de Fer and Edough massif) or giant ore bodies (e.g., Oued Amizour, El-Aouana and Aïn Barbar; Benali, 2007; Villemaire, 1987; Marignac, 1983).

Oued Amizour massif is an example of this magmatic activity that was accompanied by the emplacement of the largest Zn deposit in north Algeria. The massif has been previously studied by Semroud (1981) and Semroud et al. (1994) who presented a detailed geological framework of the igneous rocks, including petrological and mineralogical investigations. However, few geochemical data (major and trace elements) were published. The recent work of Benali (2007) who discussed the ore deposits associated with the igneous rocks of north Algeria, gave a detailed description of the Oued Amizour volcanic-hosted mineralisation and proposed a 'Kuroko-type' for the genesis of deposit.

In this paper we present new petrological and geochemical (major, trace and rare earth elements) data from the Oued Amizour igneous rocks, since few data were published on this important massif. The results are then used to infer the petrogenesis of volcanic-plutonic rocks in order to interpret their melt sources and magmatic evolution. We, then, provide, for the first time, stable S-, O- and C-isotopic composition and fluid inclusion data on the volcanic-hosted base-metal mineralisation, including gangue carbonates and sulphates, to determine the characteristics of the mineralising fluids. The petrological, geochemical, fluid inclusion and stable isotope criteria are used to advocate for, and against, magmatic–hydrothermal contributions in these supposed 'Kuroko-type' volcanic-hosted massive sulphides.

2. Geology

The Oued Amizour massif is located on the north coast of Algeria, 15 km west of the coastal Mediterranean Sea city of Bejaia and 180 km west of the capital, Algiers. It forms the western part of the Amizour – El Aouana Basin. The igneous rocks of the Oued Amizour massif intruded the Bouhatem metamorphic basement and the Baborian carbonate units, and were emplaced into Cretaceous flysch formation that is locally covered by Tertiary sediments (Fig. 2a). The Bouhatem basement, which is part of the Kabylian basement of the Alpine Belt, consists of Palaeozoic metamorphic rocks that crop out as a window through the Cretaceous flysch formation in northern part of the massif (Fig. 2a). It is composed mainly of high-grade gneisses, micaschists and marbles grouped as "Gneiss Complex" which is overlain by low-grade pelites and subordinate volcanics (Bossière and Peucat, 1985; Monié et al., 1988). These lithologies are cross-cut by quartz and pegmatite veins up to 2 m wide (Leikine, 1971, 1974; Obert, 1981). The sedimentary rocks consist of two different formations: the allochthonous flysch and the Baborian units. The allochthonous flysch formation is composed of the so-called 'Massylian flysch' of Cretaceous age and the 'Mauretanean flysch' dated Cretaceous to Eocene. They consist mainly of carbonates, shale and sandstone. The Oligocene-Miocene 'Numidian' flysch formation overlays the Massylian and the Mauretanean flysch and is composed of clays at the base and sandstone. The Baborian units are known as Brek Gouraia and Barbacha units. The Brek Gouraia unit (Fig. 2a) is composed of Triassic gypsum-bearing marls and Cretaceous carbonate formation. The Barbacha unit consists of Liassic to Cretaceous lithologies, mainly carbonates and pelitic facies (Semroud, 1981, Semroud et al., 1994).

Structurally, the Oued Amizour massif is located between two main

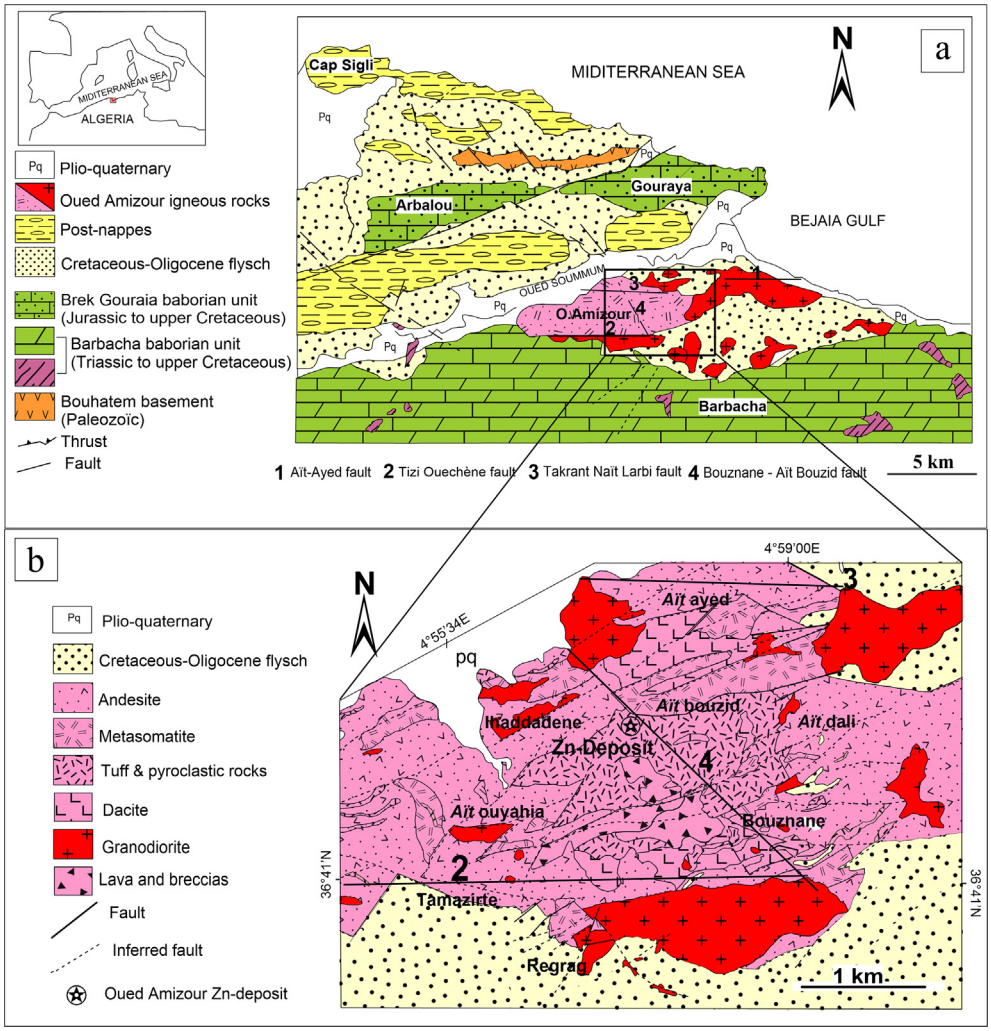

Fig. 2. (a) Geological sketch map of Bejaia-Oued Amizour region. (b) Simplified geological map of the Oued Amizour region showing the Ait Bouzid (Tala Hamza) sector (After O.R.G.M., 1998, unpub. doc.).

geological domains of north Algeria: the Internal Domain to the north comprising the Kabylian basement of Bouhatem and allocthonous flysch sediments, and the External Domain which consists of Brek-Gouraya and Barbacha Baborian units at the south (Fig. 2a). The massif itself is divided into several mining sectors: Ait Bouzid (Tala Hamza), Ihaddadene Ait Ouyahia, Tamazirte, Regrag, Bouzenane, Ait Dali and Ait Ayad (Fig. 2b). Previous studies (e.g., the mining studies carried out by the Algerian mining companies: SONAREM (Société Nationale de Recherche Minière), EREM (Entreprise de Recherche Miniére) and ORGM (Office National de Recherche Géologiques et Minières) followed more recently by the Australian WMZ (Western Mediterranean Zinc) – Terramin international company, as well as research studies, such as those of Gravelle (1959), Semroud (1981), Semroud et al. (1994), and Benali (2007)), show that the Oued Amizour igneous massif is composed of plutonic rocks located at the periphery and at the base of the igneous series, and volcanic rocks at the top. The latter are subdivided into two units: a lower unit (600– 800 m thick) composed of andesitic rocks and comprising the main Zn-ore deposit, and an upper unit consisting mainly of rhyolitic and dacitic lithologies.

The Oued Amizour massif is affected by multiple Alpine (Eocene-Miocene) fault generations; those striking ENE-WSW and NW-SE are the most important, since they are believed to be the pathways for the mineralising fluids (e.g. the Takrant Nait Larbi fault (Fig. 2a)); and younger faults striking NNE-SSW and NNW-SSE which show no relationship with the mineralisation (Gravelle, 1959; Graine and Marignac, 2001). The Tala Hamza deposit of Ait Bouzid sector, the subject of this study, is located in the central part of the volcano-plutonic massif and hosts the main massive sulphide (Zn-Pb) mineralisation. Mineralisation is characterised mainly by yellowish sphalerite occurring as a 20–30 m thick, oval ore body embedded within 'stratified' andesitic tuffs and breccias. These units are located on top of the plutonic metasomatised granodiorites (Fig. 3). The contact between the two lithologies is marked by a 10 m thick hydrothermal anhydrite layer that overlies a highly metasomatised granodioritic zone. The top contact of the anhydrite layer against the andesitic breccias and tuff is relatively sharp, whereas the base that is in contact with highly fractured and metasomatised granodiorite, often shows thin anhydrite veins and impregnations within the granodiorite. In places, anhydrite is replaced by prismatic gypsum. Subordinate mineralisation occurs also as veins and dissemination within tuffs and andesites. Emplacement of the main Zn ore body and associated Pb and Fe sulphides was accompanied by hydrothermal alteration of the host rocks, such as argillic, calcitic, chloritic, kaolinitic and sericitic alteration (Fig. 4). According to Benali (2007), the Oued Amizour mineralisation belongs to volcanic hosted massive sulphide deposits (VHMS) with some Kuroko-type signatures.

3. Petrology of the igneous rocks

Field observations and petrological studies of an approximately 800 m long drillhole that cross-cuts the whole plutonic, sub-volcanic

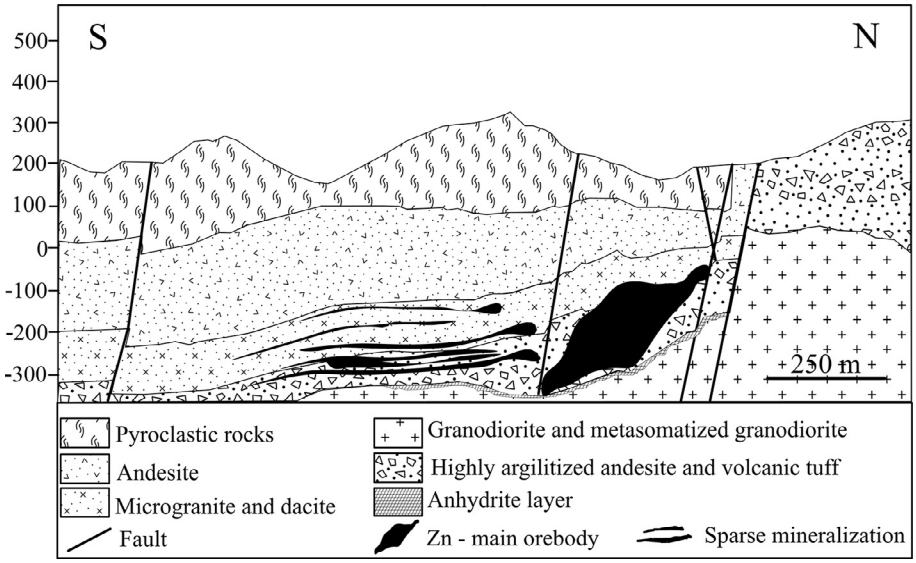

Fig. 3. Geological cross sections through the Ait Bouzid (Tala Hamza) sector showing the location of the main mineralisation.

and volcanic masses show the following lithologies from the top to the bottom: pyroclastic rocks, andesites, lavas flows, vesicular andesites, microgranites, tuff and lava flows, volcanic breccias and highly altered andesite that are intruded by aplites, metasomatised granodiorites and, finally, massive granodiorites (Fig. 4).

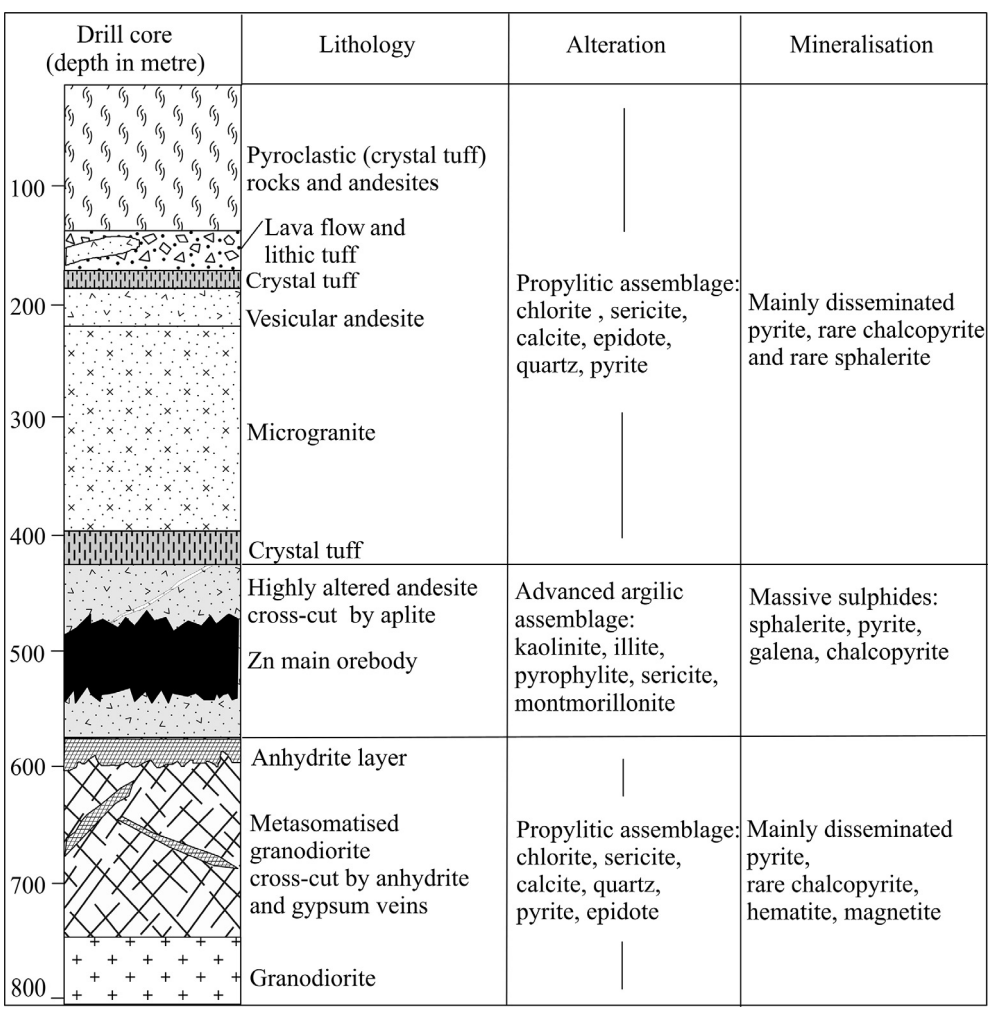

Fig. 4. Drill-core log showing the lithologies, alteration and mineralisation of Oued Amizour.

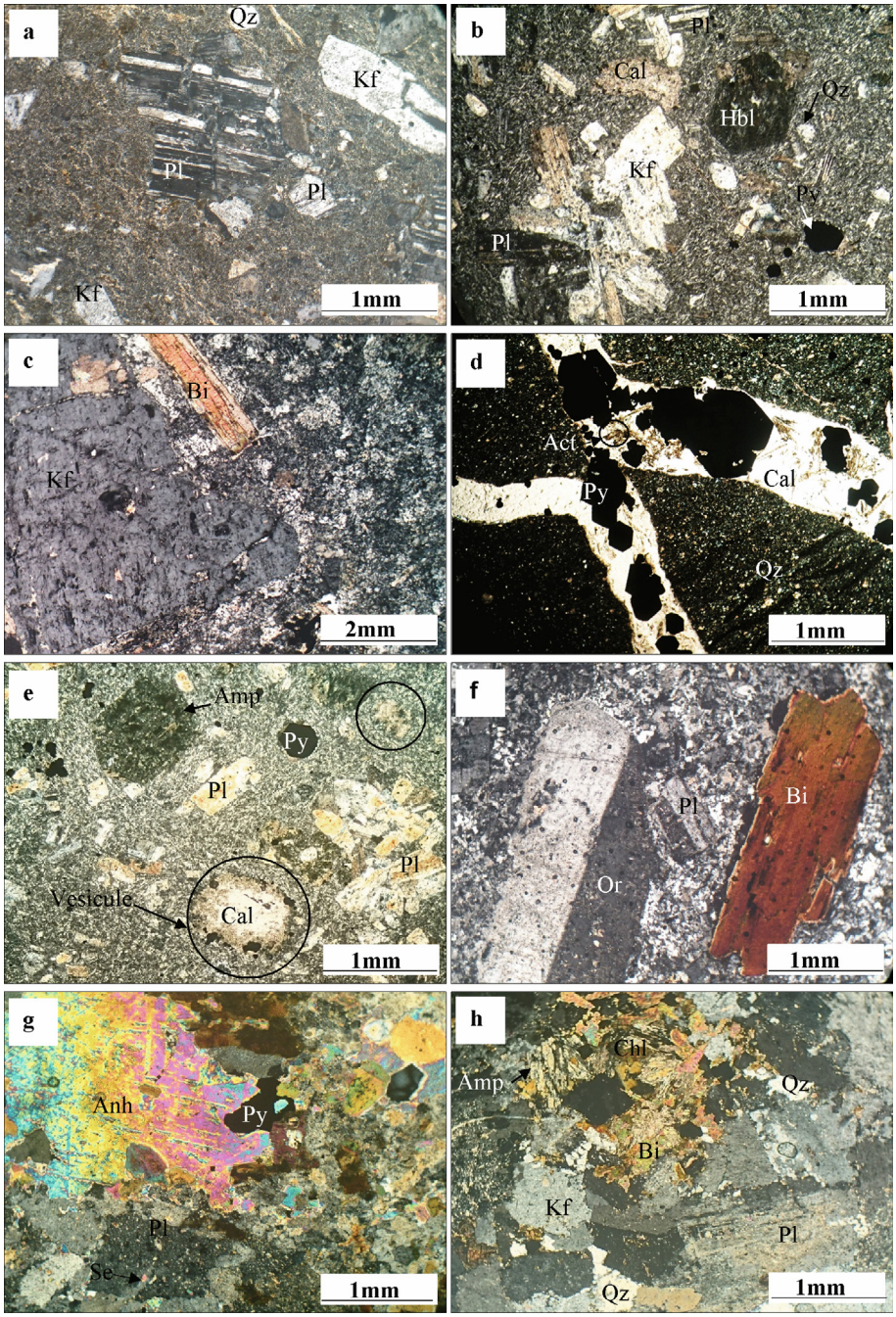

Fig. 5. Photomicrographs of the Oued Amizour granitoides: (a) pyroclastic rock, (b) andesite, (c) lava flow, (d) volcanic tuff, (e) vesicular andesite, (f) fresh microgranite, (g) metasomatised granodiorite, (h) granodiorite. (Pl: plagioclase, Or: orthoclase, Se: sericite, Chl: chlorite, Hbl: hornblende, Amp: amphibole, Cal: calcite, Qz: quartz, Py: pyrite, Act: actinolite, Kf: k-feldspar, Anh: anhydrite).

3.1. Pyroclastic rocks

The pyroclastic rocks are generally greenish gray rocks of andesitic composition and are mainly crystal tuffs which consist of quartz fragments, laths of twinned plagioclase, pseudomorphs of altered hornblende and rare K-feldspar angular grains (Fig. 5a). These crystal fragments (~0.5 to 2 mm in size) are embedded within a matrix which often shows fluidal-like textures. Subhedral pyrite minerals are often disseminated within the matrix which underwent extensive calcitic, sericitic and chloritic alteration.

3.2. Andesites

The andesites are the most abundant volcanic rocks in the Oued Amizour region. They are often porphyritic mesocratic rocks and show greenish colour when altered. The andesites (Fig. 5b) are composed mainly of twinned and zoned plagioclase phenocrysts (An_{40-55}), chloritised biotite, altered subhedral hornblende, rare quartz and K-felspar phenocrysts (mainly sanidine). The groundmass consists of microlaths of plagioclase showing a flow texture. The accessory minerals are monazite, zircon and ubiquitous, disseminated, euhedral pyrite that in places fills the microcracks of the rocks.

3.3. Lava flows

The lava flows are composed of perthitic K-feldspar phenocrysts (up to 1 mm in size) often altered to sericite, recrystallised quartz and chloritised biotite. These phenocrysts are embedded within a microlithic groundmass (Fig. 5c). Apatite and sphene crystals are the main accessory minerals, and alunite, calcite and pyrite are the common secondary minerals.

3.4. Tuff

The tuff formation is about 150 m thick and is mainly composed of lithic tuffs which exhibit grey, dark grey, to black colour. Sedimentary xenoliths are present and show various shapes; they are composed of marl and Oligocene sandstone fragments. Vitric tuff is locally stratified and often shows glassy texture, though recrystallised fine-grained (< 0.2 mm) quartz can be distinguished. The volcanic tuff formation is cross-cut by andesite dikes and calcite veins. Calcite veins, mm to cm wide, are often plugged by disseminated euhedral to subhedral pyrite and acicular actinolite crystals (Fig. 5d).

3.5. Vesicular andesites

Vesicular andesites (~30 m thick) are similar to the andesites described above; they are greenish in colour, exhibit porphyritic texture and are composed mainly of plagioclase (An_{35-45}) phenocrysts (~3 mm), chloritised hornblende, relicts of pyroxene and rare K-feldspar. Calcitisation is observed on altered plagioclase, pyroxene and hornblende. Vesicles are rounded to elongated spaces filled by calcite, quartz and pyrite (Fig. 5e).

3.6. Microgranites

The microgranites, of about 200 m thick, are strongly silicified; they are pink to pale pink in colour and consist of euhedral, often perthitic, K-feldspar phenocrysts, recrystallised quartz and chloritised biotite (Fig. 5f). Subhedral sphene and prismatic apatite are the main accessory minerals; apatite is often enclosed in biotite flakes. The groundmass is composed of microliths and microcrystals of feldspar, with both the matrix and K-feldspar phenocrysts extensively replaced by sericite and calcite. Euhedral pyrite is ubiquitous and is randomly disseminated in the rocks.

3.7. Aplites

White, metre-thick aplites veins crosscut andesitic breccias (cf. Fig. 4). They are composed of fine-grained quartz and rare K-feldspar crystals displaying granular texture. Silicification of aplite is shown by recrystallised, xenomorphic, fine-grained quartz aggregates. Fractures are filled with subhedral to euhedral pyrite, sphalerite and galena.

3.8. Metasomatised granodiorites

Metasomatised granodiorites are located between the massive plutonic granodiorite at the bottom and the highly altered andesites above (cf. Fig. 4). They are composed of quartz aggregates, K-feldspar and secondary fine-grained calcite crystals. Impregnated anhydrite crystals are also present. The granular texture of the granitoid is wholly obliterated and the rock is transformed into a metasomatite (Fig. 5g), containing euhedral disseminated pyrite grains, up to 2 mm in size. Massive anhydrite forms a layer of more than 10 m thick and is composed of cm size crystals associated in places with pyrite grains.

3.9. Granodiorite

The granodiorite forms the base of this igneous series (cf. Fig. 4). It consists of quartz aggregates, K-feldspar phenocrysts, subhedral plagioclase of oligoclase-andesine composition, and biotite (Fig. 5h). Sphene and apatite are the main accessory minerals. The rock is often fissured and the microcracks are filled with anhydrite and pyrite. Pyrite is also disseminated within the rock as euhedral, 1–5 mm grains.

4. Mineralisation

The Oued Amizour Zn-deposit is an example of many ore deposits related to the Tertiary magmatic activity in the Alpine Belt of north Algeria and is considered the largest in this zone (e.g.. Ain Barbar (Marignac, 1983); El Aouana (Villemaire, 1987); Edough (Laouar et al., 2002)). A number of exploration programs have been undertaken by Algerian mining companies (SONAREM, EREM and ORGM) since 1970, as a result of which the Tala Hamza Zn-Pb deposit was discovered. According to mineral showings that are observed at several localities, the massif was divided in a number of sectors, e.g., Ait Bouzid (Tala Hamza), Ihaddadene Ait Ouyahia, Tamazirte, Regrag, Bouzenane, Ait Dali and Ait Ayad. Recently, the Australian Terramin Company has taken over the project for further prospection and exploitation, starting with Tala Hamza deposit which is the most important with 68.6 million tonnes at 4.6% zinc and 1.1% lead in the measured, indicated and inferred resources (Terramin Australia Ltd. Report of December 2009; unpublished).

The main ore body at Tala Hamza occurs as lens-shaped body that is interbedded within the andesitic breccias and highly altered tuffs, at a depth of 400 to 500 m. The ore body, which is southerly dipping, has a thickness that varies between 30 and 200 m. The main base metal mineralisation consists of sphalerite and galena; pyrite is widespread while chalcopyrite rarely occurs. Pure sphalerite mineralisation of about 20–30 m thick shows lenticular shape within the main ore body.

The mineralisation styles range from massive through semi-massive, stockwork, breccia and disseminated sulphides. Mineralisation is often fine-grained at upper levels, but becomes medium to coarse-grained towards the main ore body. The latter consists of massive sulphides dominated by Zn sulphides (sphalerite and schalenblende), galena and Fe-sulphides (pyrite, marcassite and melnikovite). Sphalerite is characteristically a honey-yellow colour mineral. It often occurs as massive form filling the interstices of the brecciated andesites (Fig. 6a), but millimeter- to centimeter-thick veins associated with pyrite and galena can also occur within the andesitic tuffs (Fig. 6b).

Microscopically, sphalerite often shows xenomorphic, millimetric grains that are sometimes replaced by marcasite and melnikovite. The latter shows colloform structures (Fig. 7a) that are also observed on hand specimen (Fig. 6c). Schalenblende which is yellow to brownish in colour also shows colloform structures (Fig. 6b and 7b). Inclusions of galena and sphalerite often occur within schalenblende minerals (Fig. 7b). Galena occurs as (i) millimeter-thick veins of large, xenomorphic crystals (Fig. 6b), (ii) disseminations within the rock often associated with pyrite (Fig. 7c), or (iii) a space filling mineral associated with calcite (Fig. 7a). Pyrite is ubiquitous and usually occurs as disseminated grains throughout the whole volcanic pile (Fig. 6d). Occasionally, it shows zoned, space-filling aggregates (Fig. 6e) or mm wide veinlets cross-cutting the rocks (Fig. 6f). Microscopically, pyrite occurs as euhedral millimetric crystals disseminated within the rock (cf. Fig. 5e) or associated with calcite in the veinlets (cf. Fig. 5d). Rare, zoned subhedral crystals are often associated with or replaced by galena and sphalerite in the main ore body (Fig. 7c). Anhedral pyrite is sometimes associated with magnetite and chalcopyrite (Fig. 7d and e). Marcasite and melnikovite often replace pyrite aggregates; marcasite is often twinned, occurring commonly as overgrowths on subhedral to euhedral pyrite crystals, while melnikovite is more colloidal and zoned with reddish yellow colour. Chalcopyrite is rare and occurs as xenomorphic interstitial fine-grained crystals within the rocks and is usually corroded by magnetite (Fig. 7f). Sulphate minerals are mainly anhydrite with subordinate gypsum. Anhydrite is often prismatic, 1–5 mm in

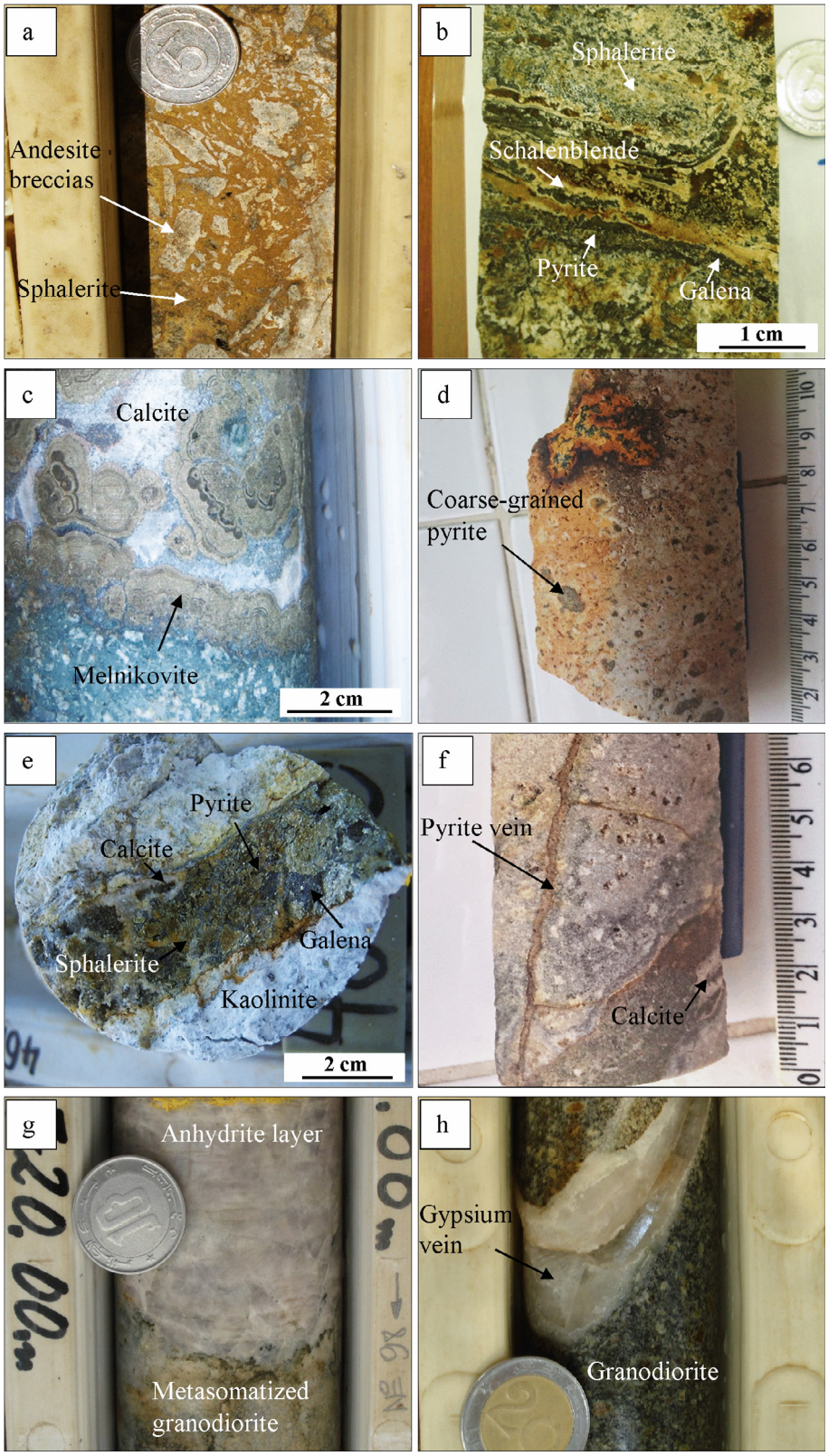

Fig. 6. Textures of the Oued Amizour mineralisation and host rocks: (a) breccia texture showing clasts of andesites cemented by massive sphalerite, (b) veins of sphalerite, scalenblende, galena and pyrite within the andesitic tuffs, (c) melnikovite colloform structure and space-filling calcite within the main ore body, (d) disseminated pyrite within the rock, (e) mineralised vein cross-cutting kaolinitised andesite and showing euhedral galena, pyrite and sphalerite cemented by calcite, (f) veinlets of pyrite cross-cutting the rock, g: massive anhydrite overlying the metasomatised granodiorite, (h) gypsum vein within the granodiorite.

size and occurs as a thick layer (Fig. 6g) underneath the main sulphide ore body. It also occurs as fine, xenomorphic, interstitial crystals within the main ore body. Gypsum often replaces anhydrite and occurs as millimeter-thick veins cross-cutting the underlying granodiorite (Fig. 6h). Iron oxides are represented by magnetite which is brownish gray and is usually fine- to medium-grained crystals, sometimes

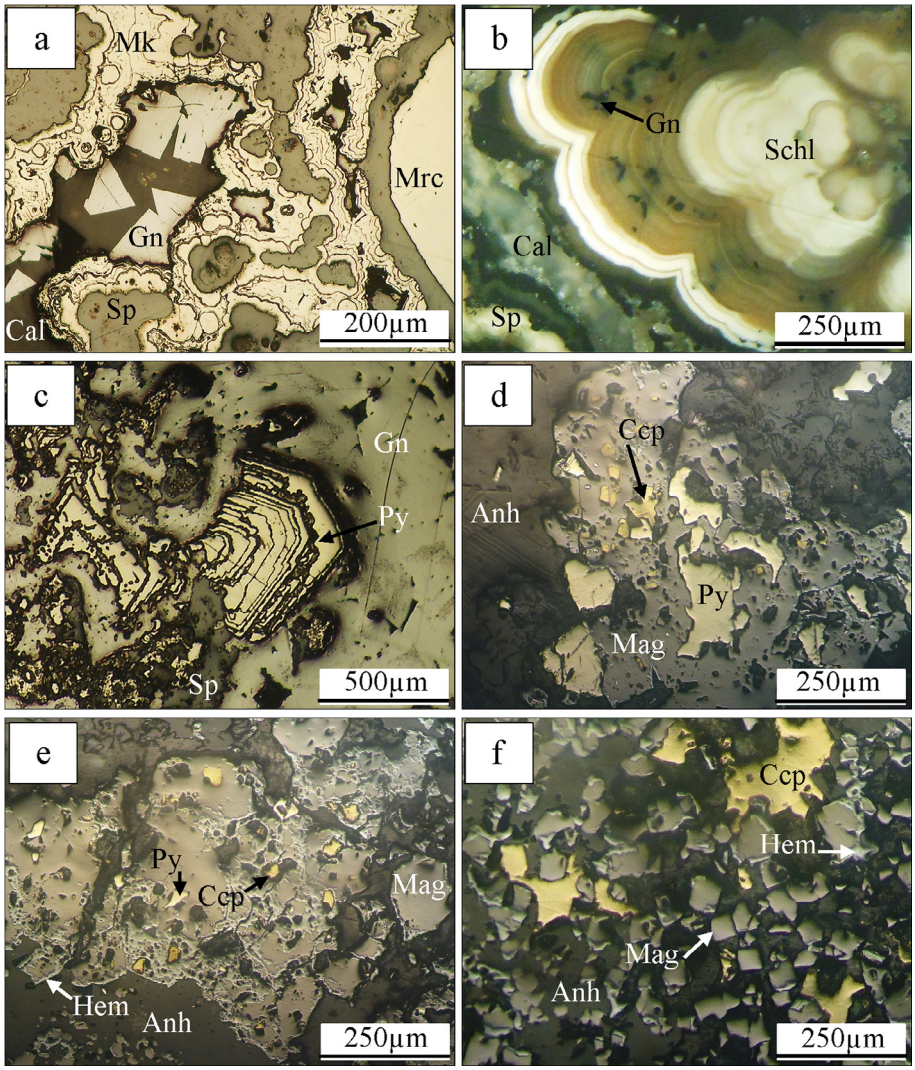

Fig. 7. Photomicrographs in reflected light showing the ore textures of Oued Amizour deposit: (a) sphalerite (Sp) replaced by marcassite (Mrc) and melnikovite (Mk); the latter shows colloform structures, (b) schallenblende (Schl) showing colloform structures and galena (Gn) inclusions; calcite (Cal) is a space-filling gangue mineral, (c) subhedral, zoned pyrite (Py) partly replaced by sphalerite and galena, (d) and (e) chalcopyrite (Ccp) and pyrite replaced by magnetite (Mag); anhydrite (Anh) is interstitial and space-filling mineral, (f) anhedral chalcopyrite replaced by magnetite; anhydrite is a space-filling mineral.

surrounded by hematite. Iron oxides usually replace pyrite and chalcopyrite (Fig. 7d–f); this replacement texture could be explained by hydrothermal processes taking place from reduced to oxidising environment in the main ore body.

The paragenetic sequence can be divided into two main hydrothermal stages followed by two alteration processes:

- Stage I characterised by the deposition of disseminated pyrite and chalcopyrite;
- Stage II in which the main minerals were deposited within the ore body. This stage started with the deposition of massive pyrite, sphalerite and galena (stage IIa), followed by the formation of pseudomorphic macasite, open space-filling melnikovite, schalenblende and the deposition of calcite and anhydrite which are interstitial minerals within the main sulphide ores (see Fig. 7). (stage IIb);
- Stage III in which anhydrite was partially transformed into gypsum;
- Stage IV characterised by oxidation processes that developed iron oxides and oxyhydroxides.

5. Alteration assemblages

The Oued Amizour igneous rocks were subjected to severe hydrothermal alteration that contributed to mineralogical and chemical changes. However, the alteration intensities differ based on rock type and depth. Fig. 4 illustrates different types of alteration and their corresponding depth. The products (mineralogy) of hydrothermal alteration were determined by petrographic examination and X-ray diffraction analysis. Alteration zoning can be clearly observed on the granitoid's lithological drill-core (Fig. 4): (i) within the metasomatised granodiorites, alteration zone is characterised by chlorite, calcite and sericite, but also quartz and pyrite; (ii) towards the main Zn orebody, an argillic assemblage is represented by kaolinite ± montmorillonite ± illite ± pyrophylite and rare sericite that characterises the brecciated andesite; (iii) towards the surface, the alteration products are mainly chlorite, sericite, calcite, pyrite and quartz, in addition to iron-oxide in the microcracks. A general feature is that alteration increases in strength from surface to depth towards the proximal zone of the Zn-Pb orebody where the argillitic assemblage becomes more abundant. Weathering, however, dominates at shallower depths.

Table 1
Major (wt%), trace (ppm) and rare earth elements (ppm) analyses of the Oued Amizour granitoids.

	Microgranites				*Aplites*		*Granodiorites*			
	029	032	036	037	069	137	105	107	159	165
SiO_2	69.70	66.71	68.30	67.50	75.20	75.10	60.50	61.50	56.60	69.80
Al_2O_3	14.90	14.70	15.75	15.50	13.45	14.90	15.20	15.95	14.75	14.35
$Fe_2O_3^t$	2.17	2.62	2.02	2.36	1.49	0.24	5.18	4.46	6.33	1.44
CaO	0.74	1.34	0.77	0.77	0.44	0.43	2.20	3.03	5.54	1.98
MgO	1.47	1.07	1.69	1.97	0.26	0.05	3.94	3.86	4.42	1.23
Na_2O	1.33	3.16	3.54	3.24	4.45	8.51	3.56	4.08	3.86	6.86
K_2O	7.69	5.94	6.12	6.20	0.62	0.18	4.37	2.99	2.83	0.42
TiO_2	0.46	0.45	0.48	0.64	0.24	0.04	0.72	0.73	0.66	0.42
MnO	0.03	0.04	0.03	0.05	0.01	< 0.01	0.04	0.04	0.03	0.06
P_2O_5	0.10	0.08	0.08	0.11	0.04	0.06	0.18	0.17	0.27	0.13
LOI	2.91	2.37	2.42	2.31	3.58	0.83	3.03	1.40	4.08	2.37
Total	*101.61*	*98.48*	*101.27*	*100.71*	*99.79*	*100.37*	*98.97*	*98.26*	*99.43*	*99.07*
Ba	861	290	448	53	27	17	299	181	173	23
Cr	9	6	9	9	9	9	10	10	20	9
Cs	10	–	8	7	8	1	10	10	13	3
Ga	18	–	21	21	14	6	19	20	20	17
Hf	9	–	8	13	5	4	8	7	5	6
Nb	16	15	14	17	10	1	15	10	9	1
Rb	455	416	388	422	49	10	266	227	247	34
Sr	105	117	133	128	108	230	181	247	312	130
Ta	2	–	2	2	1	–	1	1	1	1
Th	34	28	30	33	35	2	26	19	25	22
V	38	41	45	54	22	4	98	108	245	59
Y	30	23	24	26	11	2	40	23	33	13
Zr	334	81	301	499	165	176	291	251	217	217
Ce	82	55	64	77	14	4	103	55	72	28
Dy	5	4	4	4	2	–	7	4	6	2
Er	3	2	2	3	1	–	5	3	3	1
Eu	1	1	1	1	1	–	1	1	1	1
Gd	5	4	2	4	1	–	7	4	6	2
Ho	1	–	1	1	1	–	1	1	1	1
La	39	27	33	42	7	2	49	30	33	14
Lu	1	–	1	1	1	–	1	–	1	–
Nd	32	–	24	27	5	2	44	23	31	11
Pr	8	22	6	7	1	–	11	6	8	3
Sm	6	4	5	5	1	–	8	4	6	2
Sn	8	–	9	9	7	2	13	10	9	8
Tb	1	–	1	1	–	–	1	1	1	–
Tm	1	–	1	1	–	–	1	–	1	–
U	27	–	21	21	17	2	26	12	11	13
W	7	–	1	2	–	–	2	1	1	4
Yb	4	2	3	3	2	–	5	3	3	2

Pyroclastites. andesitic lava and volcanic tuff of Oued Amizour

	005	011E	014	016E	022	24	049	055	058	122	122E	125
SiO_2	67.80	64.00	59.40	52.90	57.10	57.90	58.20	64.20	61.80	57.70	55.30	72.70
Al_2O_3	15.00	16.85	17.45	17.00	14.35	16.30	18.20	15.50	16.80	20.20	17.85	13.60
$Fe_2O_3^t$	2.46	3.03	4.69	11.55	9.06	6.30	4.80	5.14	4.85	4.19	7.26	2.39
CaO	1.32	2.19	2.72	0.33	2.36	0.95	1.16	0.22	1.16	0.67	1.34	0.25
MgO	1.79	1.94	2.05	3.06	4.98	6.46	3.55	1.63	3.09	2.24	4.63	1.00
Na_2O	2.67	5.59	4.06	2.50	4.51	3.06	4.93	0.11	0.41	0.62	6.56	0.16
K_2O	3.61	1.81	3.20	3.50	0.60	2.50	3.64	5.48	4.21	8.20	0.19	4.18
TiO_2	0.45	0.68	0.54	0.69	0.69	0.73	0.86	0.75	0.77	1.00	0.72	0.66
MnO	0.03	0.04	0.05	0.05	0.06	0.10	0.08	0.01	0.05	0.03	0.10	0.01
P_2O_5	0.07	0.10	0.12	0.12	0.15	0.15	0.19	0.09	0.15	0.18	0.11	0.14
LOI	4.94	4.00	5.23	8.37	5.70	5.05	4.29	6.21	6.88	5.32	5.20	5.80
Total	*100.18*	*100.31*	*99.58*	*100.09*	*99.60*	*99.50*	*99.97*	*99.35*	*100.18*	*100.42*	*99.31*	*100.92*
Ba	236	214	168	120	88	639	335	136	121	525	20	232
Cr	9	320	200	30	110	43	40	10	10	30	260	100
Cs	11	8	16	27	5	–	5	29	37	20	1	34
Ga	18	14	18	26	23	–	22	30	25	24	18	20
Hf	8	2	2	3	3	–	5	7	7	3	2	3
Nb	16	5	5	5	14	8	10	13	13	6	4	13
Rb	305	132	279	372	31	116	204	596	492	672	12	324
Sr	88	213	168	42	148	162	137	8	24	54	194	31
Ta	2	1	1	1	1	–	1	1	1	1	1	1
Th	32	5	6	6	10	13	18	24	23	7	5	10
V	37	91	142.	212	161	147	141	110	127	279	134	239
Y	21	12	13	15	28	21	21	29	25	17	23	22

(*continued on next page*)

Table 1 (*continued*)

Pyroclastites. andesitic lava and volcanic tuff of Oued Amizour

	005	011E	014	016E	022	24	049	055	058	122	122E	125
Zr	298	88	86	95	130	167	212	272	272	121	89	122
Ce	87	27	21	54	221	56	45	19	70	13	101	7
Dy	4	2	2	2	5	3	4	5	4	3	4	4
Er	2	1	2	2	3	2	2	3	3	2	2	3
Eu	1	1	1	1	2	1.	1	1	1	1	1	1
Gd	4	2	2	2	7	4	4	3	4	3	4	4
Ho	1	1	1	1	1	–	1	1	1	1	1	1
La	44	15	12	29	140	30	22	9	35	5	55	3
Lu	1	–	–	–	–	–	–	1	–	–	–	–
Nd	31	12	10	18	69	–	20	9	28	8	30	6
Pr	9	3	2	5	20	23	5	2	7	2	9	1
Sm	5	2	2	3	9	4	4	2	6	3	5	3
Sn	7	8	6	21	7	–	5	28	28	8	4	5
Tb	1	–	–	–	1	–	1	1	1	1	1	1
Tm	–	–	–	–	–	–	–	1	–	–	–	–
U	17	4	5	8	5	–	12	11	10	6	4	6
W	2	9	5	4	2	–	3	8	6	13	9	4
Yb	3	1	2	2	3	2	2	4	3	2.	2	3

$Fe_2O_3^t$: Total iron.

6. Analytical techniques

Various igneous lithologies were sampled from a representative bore-hole (about 800 m deep) that was recently drilled by WMZ (Western Mediterranean Zinc Company) (cf. Fig. 4). The bore-hole is located at the central part of the Oued Amizour Zn deposit and cross-cuts the whole volcanic-plutonic pile. About 120 samples were collected for the present study.

Based on detailed petrographical investigation, only 22 samples, including three enclave specimens (011E, 016E and 122E) from the volcanic breccias and tuff formation, were selected among the least altered lithologies for geochemical analyses. The samples were trimmed to centimeter-size grains and sent to ALS Minerals, Seville, Spain, for major, trace and rare earth element analysis. Prepared samples were analysed using ICP-AES and ICP-MS for major and trace elements respectively. The results are summarized in Table 1.

Fluid inclusion study was carried out on anhydrite and calcite samples from the stage II of the main mineralisation. The anhydrite sample was collected from the massive anhydrite layer just underneath the main Zn-ore body, whereas the calcite sample is the gangue mineral of the main sulphide mineralisation. Doubly polished rock wafers (less than 1 mm thick) were used for microthermometric measurements of primary fluid inclusions at the 'Laboratoire de Minéralogie et Géochimie Appliquée, Faculté des Sciences, Université El Manar, Tunis', using a Linkam THMS G600 heating-freezing stage, with a temperature range between −180 and +600 °C (Roedder, 1984a). If fluid inclusions within individual clusters showed dissimilar homogenisation temperatures, they were likely stretched, and the microthermometric data were discarded. The obtained data reasonably and sufficiently characterise both the anhydrite layer and ore formation conditions because mineralisation was uniformly developed throughout this zone of the Oued Amizour deposit at this stage.

For sulphur isotope study, 22 sulphide samples including pyrite, sphalerite and chalcopyrite were prepared (7 samples from the volcanic upper unit, 7 samples from the main ore body and 8 samples from the plutonic rocks). For sulphates, 10 samples were selected: 7 anhydrite and 3 gypsum samples collected from the veins at the transition zone between the plutonic and volcanic rocks, just below the main ore body. For carbonate carbon and oxygen isotope studies, twelve (12) gangue calcite samples were collected from the whole volcanic pile, including the main ore body. In all cases, calcite occurs as white, spathic crystals of 0.5–1 cm. Pure minerals were separated by careful handpicking techniques under a binocular microscope then cleaned using bi-distilled water.

Stable isotope analyses were carried out at the Scottish Universities Environmental Research Centre, East Kilbride, Glasgow, UK. For S isotope analysis, SO_2 gas was produced from both sulphides and sulphates following the standard technique of Robinson and Kusakabe (1975) and $^{34}S/^{32}S$ ratios were determined on a VG Isogas Sira 2 mass spectrometer. Results are reported in the standard "delta" (δ) notation as per mil (‰) deviations relative to Cañon Diablo Troilite (V-CDT) standard. Analytical reproducibility is ± 0.2‰ at 1σ; NBS 123 gives −17.1‰ and IAEA –S-3 −32.1‰.

For carbonate O and C isotope analyses, the sample powders were converted to CO_2 by reacting with phosphoric acid (H_3PO_4) 100% at 25° C (McCrea, 1950). The isotope analysis of oxygen and carbon of prepared CO_2 was carried out on a separate VG Sira 2 mass spectrometer according to the method described by Craig (1957, 1965). Results are expressed in per mil (‰) relative to V-PDB standard for carbon and V-SMOW for oxygen. Reproducibility is ± 0.2‰ or better at 1σ and standardisation is via NBS 19.

7. Results

7.1. Rock geochemistry

The selected samples for chemical analyses are considered the least altered rocks, though the loss on ignition (LOI) contents may reach 5% in the intermediate to mafic volcanic rocks which often show traces of calcitisation (see Fig. 5). Samples that show LOI more than 5% are considered hydrothermally altered and are therefore excluded from the discussion of magmatic evolution. The entire geochemical data are summarized in Table 1.

The SiO_2 concentrations of all granitoids, including mafic enclaves, range from 52.9 to 75.2 wt%. The Na_2O and K_2O contents in the altered rocks show the effect of post magmatic alteration; e.g. Na_2O contents in the aplites are very low (> 1%) compared to K_2O which shows high values (up to 8%). However, these classic mobile elements exhibit a magmatic behaviour in the less altered rocks.

7.2. Fluid inclusions

All observed primary fluid inclusions contain two phases: liquid and vapour (Fig. 8). These inclusions show variable forms but most of them are rectangular, and their sizes vary from 5 to 30 μm. The vapour phase is often spherical and represents 5–20% of the whole inclusion.

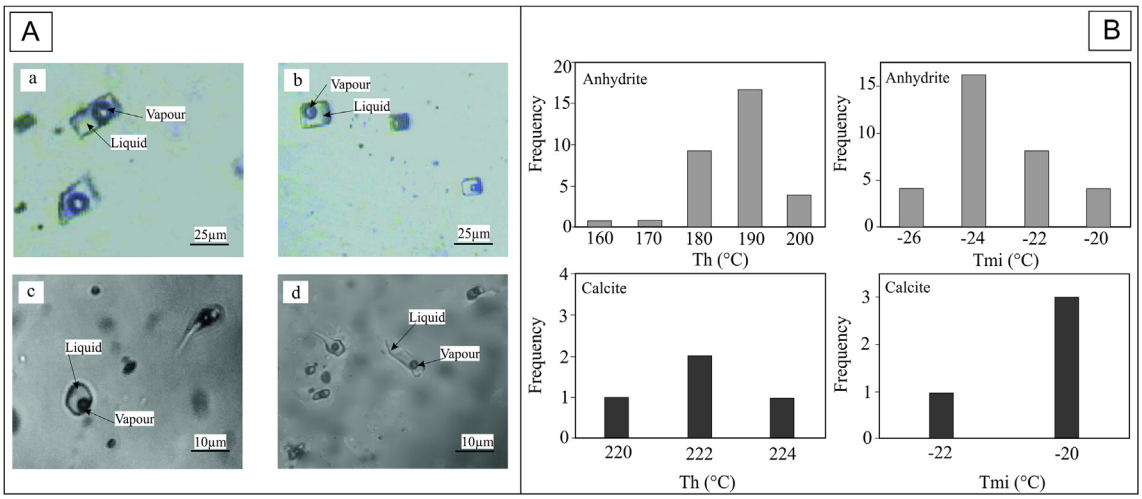

Fig. 8. A: Photomicrographs of fluid inclusions hosted in anhydrite (a and b) and calcite (c and d) from the Oued Amizour ore deposit. B: Histograms of thermometric measurements on anhydrite and calcite. Th: homogenisation temperature; Tmi: melting temperature of ice.

Major concerns are often associated with analyzing fluid inclusions in anhydrite, including (i) potential stretching (Bodnar and Bethke, 1984), (ii) partial dissolution, and (iii) precipitation during heating and formation of gypsum from reaction of anhydrite with the trapped aqueous fluid (Le Bel and Oudin, 1982). Nevertheless, the consistency of the measured homogenisation temperatures and salinity results in anhydrite samples along with the similarity of these data to those obtained in calcite samples from similar depths in the main ore body, argue against the influence of any of the above factors.

The microthermometric data obtained from the observed primary inclusions are presented in Table 2. Homogenisation temperatures (Th) range from 170 to 202 °C, with a maximum frequency at 190 °C for anhydrite and 220 to 224 °C with a peak at 222 °C for calcite (Fig. 8).

Eutectic temperatures of inclusions in all cases were below that of the eutectic NaCl-H_2O system (−20.8 °C); they are between −32.8 and −60 °C. Usually, these temperatures are attributed to the presence of other divalent cations, such as Na^+, Ca^{++} and Mg^{++} and are characteristic of H_2O-NaCl-$CaCl_2$ ternary system (Borisenski, 1977; Crawford, 1981; Roedder, 1984b). Salinities are determined by combining the melting temperatures of hydrohalite (Thh) with the corresponding melting temperature of ice (Tmi). The computer programme of Chi and Ni (2007) was used to determine the salinity. At Oued Amizour Zn-deposit, the latter varies between 22.3 and 26.6 wt% eq. NaCl for anhydrite fluid inclusions and from 22.3 to 23.0 wt% eq. NaCl for calcite (Table 2).

Table 2
Data of fluid inclusion microthermometric measurements in anhydrite and calcite of the Oued Amizour ore deposit. Th: homogenization temperature (°C); Te: eutectic temperature (°C); Tmi: melting temperature of ice (°C); Sal: salinity (wt.% eq. NaCl);

	Anhydrite				Calcite			
	Te	Tmi	Th °C	Sal	Te	Tmi	Th	Sal
1	−43.0	−20.3	189.1	22.3	−60	−21	220	23
2	−45.0	−23.5	200.0	24.3	−58	−20	222	22.3
3	−38.0	−24.7	201.0	24.9	−57	−21	223	23
4	−45.0	−22.0	182.0	23.6	−55	−21.5	224	23
8	−43.0	−22.3	189.9	23.6				
9	−36.0	−25.7	202.0	25.5				
10	−34.0	−24.4	188.0	24.9				
11	−35.0	−20.2	194.0	22.3				
12	−33.0	−21.8	184.7	23.0				
13	−39.0	−25.0	190.2	25.5				
14	−36.0	−24.1	197.3	24.9				
15	−44.0	−25.0	189.2	25.5				
16	−40.3	−23.0	199.0	24.3				
17	−42.0	−25.8	192.0	25.5				
18	−45.0	−25.6	196.6	25.5				
19	−32.8	−22.2	194.6	23.6				
20	−33.4	−23.3	193.0	24.3				
21	−35.0	−25.1	190.1	25.5				
22	−40.9	−26.5	189.7	26.6				
23	−38.9	−26.3	191.1	26.6				
24	−39.1	−25.7	191.3	25.5				
25	−34.5	−25.8	198.6	25.5				
26	−41.0	−23.9	190.0	24.3				
27	−41.0	−25.5	192.5	25.5				
28	−40.0	−24.9	198.1	24.9				
29	−35.0	−24.5	169.9	24.9				
30	−40.0	−26.1	202.0	26.6				
31	−38.0	−25.0	196.6	25.5				
32	−37.0	−22.6	192.3	23.6				

7.3. Stable isotopes

Sulphur isotope measurements were carried out on sphalerite, chalcopyrite and pyrite separates from the main Zn deposits and different igneous lithologies described above, and the results are presented in Table 3 and Fig. 9. $\delta^{34}S_{V\text{-}CDT}$ of sulphides varies between −7.2‰ and +4.5‰ (n = 22; mean = −1.3‰). There is no significant spatial variation in sulphur isotopic composition in the sulphides. Also, the distribution of the isotopic composition of sulphur from the sulphides is not closely related to their spatial distribution in the deposit. However, larger values interval is observed within the main ore deposit ($\delta^{34}S$ varies between −5.6 and +1.4‰ (n = 7)). The $\delta^{34}S$ of sulphate minerals (anhydrite and gypsum) are higher ranging from +13.2‰ to +20.6‰ (n = 10; mean = +16.3‰). The lowest values are observed within the anhydrite layer close to the main Zn ore.

Oxygen and carbon isotope results of the twelve gangue calcite samples are shown in Table 4. Analyses gave $\delta^{18}O_{V\text{-}SMOW}$ values varying between +11.2 and +20.2‰ (mean = +16.7‰) and $\delta^{13}C_{V\text{-}PDB}$ values ranging from −3.7 to −11.0‰ (mean value = −7.8‰).

8. Discussion

The SiO_2 concentrations of the Oued Amizour igneous rocks and associated enclaves vary between 52.9 and 75.2 wt% indicating that they span the range of compositions from intermediate to acidic lithologies, with the enclaves being the most mafic lithologies. On the total alkali ($Na_2O + K_2O$) vs. silica (SiO_2) (TAS-IUGS) classification diagram of Le Maitre (2002), the Oued Amizour volcanic and their

Table 3
Results of sulphur isotope analyses of the Oued Amizour mineralization.

Sample		$\delta^{34}S_{V\text{-}CDT}$ (‰)	Comments
Volcanites	*sulphides*		
O16	py	−0.1	Millimitric pyrite veins
O22	py	−2.7	Disseminated pyrite within calcite veins within tuff
O23	py	+0.3	Millimitric pyrite veins
O27a	sph	−2.2	Fine-grained sphalerite
O27b	sph	−2.7	Coarse-grained spalerite
O31	cp	−1.5	Space filling fine grained chalcopyrite
O44	sph	+4.5	Space-filling sphalerite (geodic)
Main orebody			
O69	py	−0.7	Veins of pyrite within metasomatite
O70	cp	+1.4	Massive chalcopyrite
O70	sp	−2.2	Collomorphic sphalerite
O70	py	+1.9	Massive pyrite
O75	sp	−4.0	Powder-like sphalerite
O77	sp	−5.6	Massive sphalerite
O77	py	+1.2	Massive pyrite
Plutonites			
O84	Py	+2.6	Pyrite associated with gypsum veins
O88	cpy	+2.4	Massive chalcopyrite
105	py	+3.0	Disseminated pyrite
135	py	−1.7	Coarse-grained pyrite in brecciated rock
136	cpy	−6.9	Massive chalcopyrite
136	py	−2.0	Massive pyrite
138	py	−7.2	Massive pyrite
161	py	−6.2	Disseminated pyrite within anhydrite veins
Plutonites	*sulphates*		
O84	gy	+14.7	Gypsum vein
O87	anhy	+13.2	Anhydrite disseminations
O98	anhy	+14.1	Anhydrite vein
104	anhy	+20.6	Anhydrite vein
105	gy	+19.3	Gypsum vein
153	anhy	+17.1	Anhydrite vein
155	anhy	+16.0	Anhydrite vein
157	anhy	+14.2	Meter thick anhydrite vein
161	anhy	+15.0	Cm thick anhydrite vein
166	gy	+18.7	Gypsum vein

equivalent sub-volcanic and plutonic rocks plot in the field of basaltic trachyandesite (the mafic enclaves), trachyandesite, andesite, trachydacite, dacite and rhyolite (Fig. 10a). The AFM diagram (Fig. 10b) of Irvine and Baragar (1971) shows the calc-alkaline character of the Oued Amizour granitoids. On the SiO_2 against K_2O diagram of Peccerillo and Taylor (1976), the majority of samples display high-K calc-alkaline to shoshonitic character; few samples plot in the low-K tholeiitic field (Fig. 10c). These features are similar to those of the majority of the Miocene magmatic rocks of northeastern Algeria (see: Fougnot, 1990; Ahmed-Said et al., 1993; Semroud et al., 1994; Ouabadi, 1994; Fourcade et al., 2001; Laouar et al., 2005).

Table 4
Carbon and oxygen isotopic composition of gangue calcite from Oued Amizour Zn deposit.

Sample	$\delta^{13}C_{V\text{-}PDB}$ (‰)	$\delta^{18}O_{V\text{-}SMOW}$ (‰)
016ca	−8.2	16.2
19ca f	−9.1	11.2
023caf	−6.5	15.3
026ca g	−11.	20.1
027ca g	−9.6	20.2
034ca g	−8.9	16.01
037ca	−9.1	17.9
44ca	−9.6	16.8
060ca	−7.4	12.7
136ca	−6.4	16.8
138ca	−4.5	18.5
144ca	−3.7	19.1

The variation of incompatible elements with SiO_2 contents shows the usual positive correlation (Fig. 11). On the other hand, CaO, Al_2O_3 and compatible elements, such as total iron ($Fe_2O_3^t$) and MgO show the common negative correlation with SiO_2.

On the chondrite-normalised multi-element and REE diagrams (Fig. 12), both the volcanic and plutonic lithologies show similar patterns: enrichment in large ion lithophile elements (LILE) and light rare earth elements (LREE) with respect to high field strength elements (HFSE) and heavy rare earth element (HREE) respectively. These high-K calc-alkaline rocks also have pronounced Nb and Sr negative anomalies and slight negative Eu anomaly (Fig. 12).

Ba, Rb and Sr are classic LILE that replace K and Ca in the common igneous major mineral phases such as feldspars and micas; their behavior can be used to model the role of these minerals on the evolution of granite magmas (e.g., Taylor, 1965). During granite magma

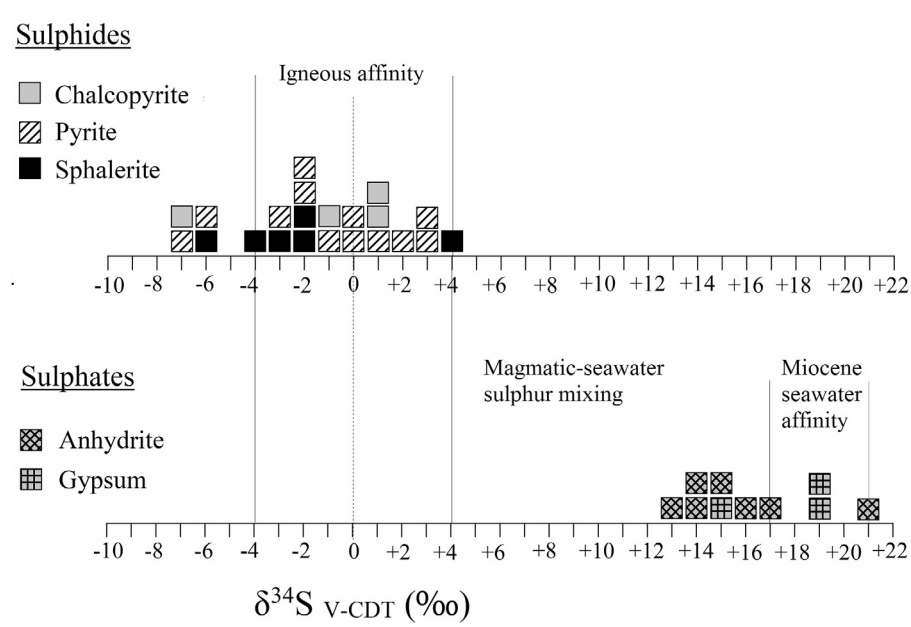

Fig. 9. Histogram showing the sulphur isotopic compositions of the Oued Amizour sulphides and sulphates.

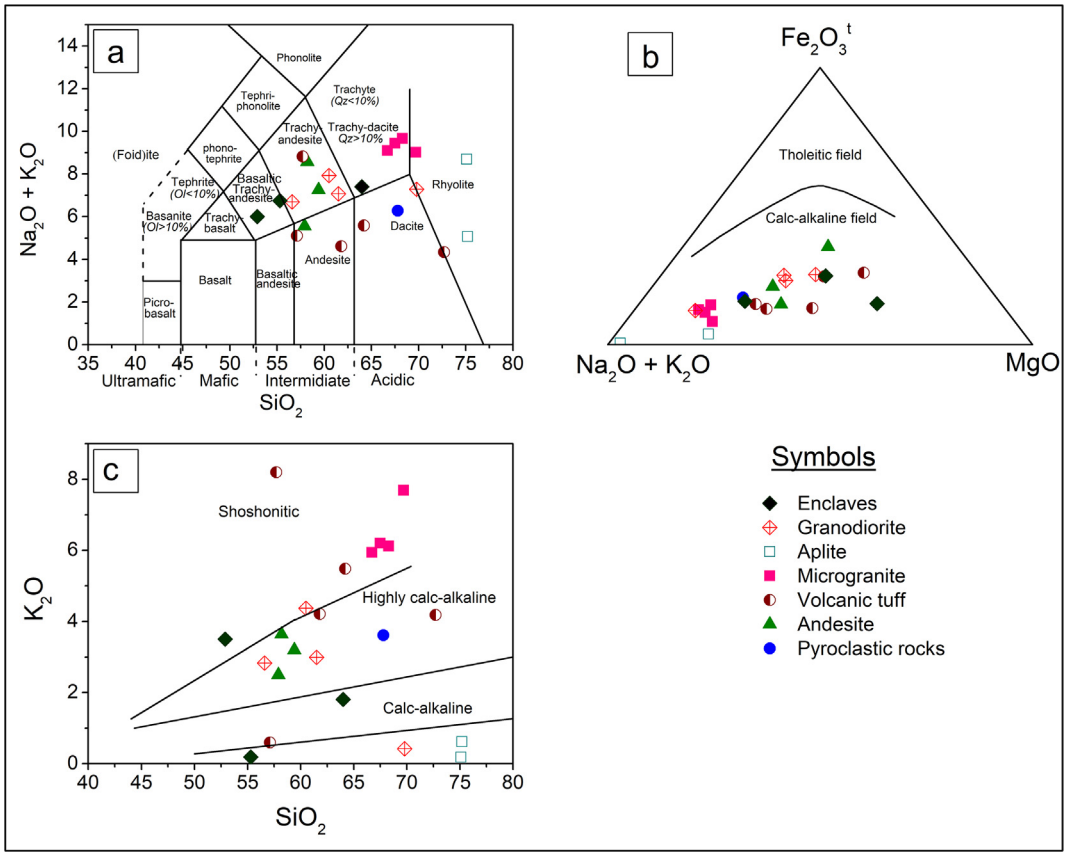

Fig. 10. a: Total alkali-silica (TAS) plot with IUGS fields after Le Maitre (2002) for the Oued Amizour granitoids; b: AFM diagram of Irvine and Baragar (1971) showing the calc-alkaline character; and c: K_2O vs SiO_2 plot of Peccerillo and Taylor (1976) showing the high-K to shoshonitic, calc-alkaline features of the Oued Amizour granitoids.

fractionation, Sr, similarly to Eu, is often the first to have a compatible behavior, as a result of plagioclase removal; it is followed by Ba which is taken into the K-feldspar structure, whereas Rb remains relatively incompatible until the last more felsic differentiates, unless the magma is hydrous enough to stabilize biotite and/or muscovite earlier on (e.g., Taylor, 1969; Culbert, 1972). Almost all the Oued Amizour igneous lithologies show negative Eu anomalies, with the most acidic cases showing the most pronounced anomaly (Fig. 12). This is systematically accompanied by Sr negative anomalies which can be explained by fractional crystallization of plagioclase either in magma chamber or during magma ascent (Wilson, 2007). This is supported by the observed negative correlations between CaO, Al_2O_3, and SiO_2 (Fig. 11). The Eu, Sr and Nb negative anomalies and the high LILE enrichment observed in the whole igneous suite indicate that the various volcanic and plutonic rocks are genetically related. They are also common characteristics of the high-K calc-alkaline series of active continental margins. Nb and Ta negative anomalies along with LREE and LILE enrichment point to a 'subduction-related signature' for the genesis of the Oued Amizour magmas. On the other hand, the presence of mafic to intermediate rocks comprising sulphides with S-isotopic signature close to that of the mantle (see below), suggest the involvement of subduction-metasomatised mantle material in the genesis of the magmas. The Nb + Y versus Rb diagram of Pearce et al. (1984) (Fig. 13) confirms that the Oued Amizour granitoids belong to the Miocene post-collisional magmatic events. This was already proposed by Fourcade et al. (2001) and Laouar et al. (2005) when studying the post-collisional Miocene igneous rocks of north-eastern Algeria. Recently, Chazot et al. (2017) pointed out that the Kabylian subcontinental lithospheric mantle previously metasomatised during the Paleogene subduction of the Tethys oceanic lithosphere is the most likely source region for the post-collisional magmas of northeastern Algeria.

The $\delta^{34}S$ values of Oued Amizour sulphide minerals vary from −7.2 to +4.9‰ (n = 22; mean = −1.3‰). The mean value of −1.3‰ is ~23‰ lower than that of coeval Miocene seawater sulphates (+22‰; Paytan et al., 1998), whereas the sulphate minerals (anhydrite and gypsum) exhibit significantly higher values (+13.2 to +20.6‰). The lowest sulphate values are recorded in the anhydrite layer close to the main ore deposit, whereas the highest values, approaching those of coeval Miocene seawater sulphates, are observed in the anhydrite veins within the metasomatised granodiorite. The range of $\delta^{34}S$ values of Oued Amizour sulphides overlaps that of sulphides recorded in igneous rocks of mantle origin ($\delta^{34}S$ ranges from −3 to +3‰; Sakai et al., 1984; Ohmoto, 1986; Taylor, 1987), with few values outside the igneous range, especially within the main mineralised zone. From these data, two major sources of sulphide-sulphur are envisaged: (1) sulphur was derived from partial inorganic reduction (thermochemical process) of marine sulphate combined with dissolution of rock sulphur as seawater convected through the volcanic andesitic breccia and tuff underlying the main ore body; a well known process in most VHMS deposits (e.g., Sasaki, 1970; Solomon et al., 1988); and (2) sulphur originates from magmatic–hydrothermal fluids (Ohmoto et al., 1983; Solomon et al., 1988), where disproportionation of magmatic SO_2 to form aqueous sulphate and H_2S according to the reaction (Huston et al., 2011):

$$4SO_{2(g)} + 4H_2O_{(l)} = 3HSO_4^- + H_2S_{(aq)} + 3H^+$$

Huston et al. (2011) pointed out that the highly acidic fluids produced by this process contribute to the formation of advanced argillic alteration assemblages, and that this reaction is significant at temperatures below 400 °C in oxidised magmatic-hydrothermal fluids.

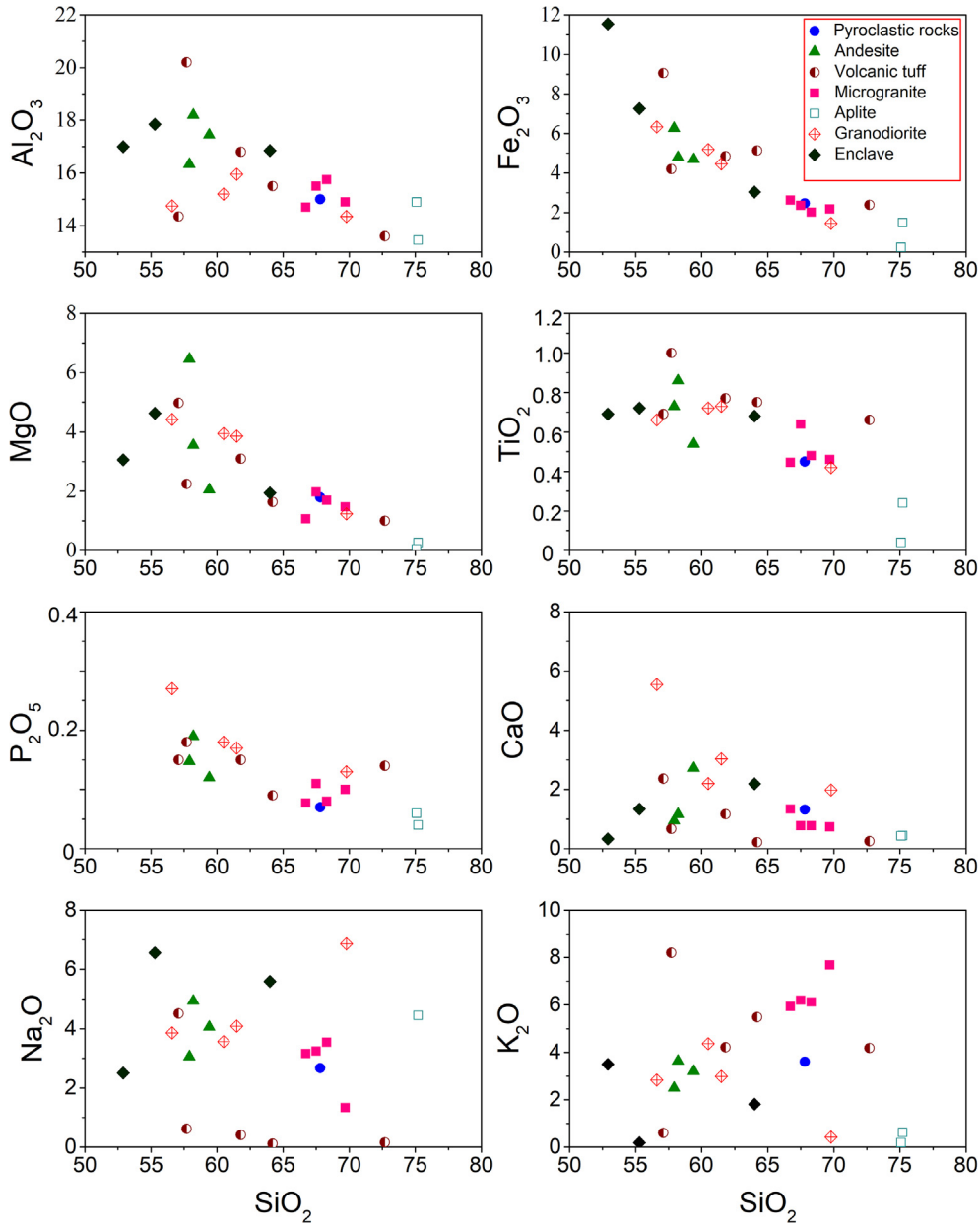

Fig. 11. Harker diagrams of major oxides versus SiO_2 (wt.%) of Oued Amizour granitoides: (sample symbols as in Fig. 10).

Under these conditions, sulphur isotope fractionation between sulphates and H_2S ($\Delta^{34}S_{sulphate-H2S}$) becomes significant; it varies from 18‰ at 400 °C to 29‰ at 200 °C (Ohmoto and Rye, 1979). Furthermore, Arribas (1995) noted that, in high-sulphidation epithermal deposits, disproportionation of magmatic–hydrothermal fluids resulted in $\Delta^{34}S_{sulphate-sulphide}$ of 20–30‰, with sulphide minerals commonly having $\delta^{34}S$ values between −10‰ and 0‰.

The range of $\delta^{34}S$ values of Oued Amizour sulphides is in agreement with the data observed in most VHMS deposits (e.g., Franklin et al., 1981; Gemmell and Large, 1992; Cook and Hoefs, 1997; Ohmoto and Goldhaber, 1997; Gemmell and Fulton, 2001; Sharman et al., 2015; Torró et al., 2016). These values can be assigned to: (a) sulphur sourced from underlying magmatic rocks; (b) thermochemically reduced seawater sulphate; or (c) a combination of both sources. The relatively large range of variation in $\delta^{34}S$ values of sulphides within the main ores (between −5.6 and + 1.9‰) along with the presence of argillic alteration and the narrow range of $\delta^{34}S$ variation within the whole 800 m borehole (between −2.7 and +4.5‰; Fig. 14) indicates that the significant source of sulphur is of magmatic origin. Both disproportionation of magmatic-hydrothermal fluid alluded to by Huston et al. (2011), and dissolved rock sulphide processes, are most likely, since they give similar sulphur isotopic compositions (Ohmoto and Rye, 1979; Ohmoto and Goldhaber, 1997; Huston et al., 2011).

The presence of the anhydrite layer and veins underneath the Zn-mineralised zone of the Oued Amizour deposit are distinctive features of the Kuroko type deposits (e.g., Lambert and Sato, 1974; Farrell and Holland, 1983; Shikazono et al., 1983; Ohmoto, 1996). According to petrological observations, anhydrite is considered to be precipitated before gypsum which clearly replaces anhydrite (see the Geology section above). This is also a feature of the Kuroko deposits, where Matsubaya and Sakai (1973), Ogawa et al. (2007) and Yeats et al. (2017) pointed out that gypsum is considered to be a secondary mineral that was formed by hydration of anhydrite. Moreover, it is considered that the anhydrite in the Kuroko-type deposits is formed by the subseafloor mixing of hydrothermal solution with seawater (e.g., Shikazono et al., 1983; Teagle et al., 1998; Chiba et al., 1998; Ogawa

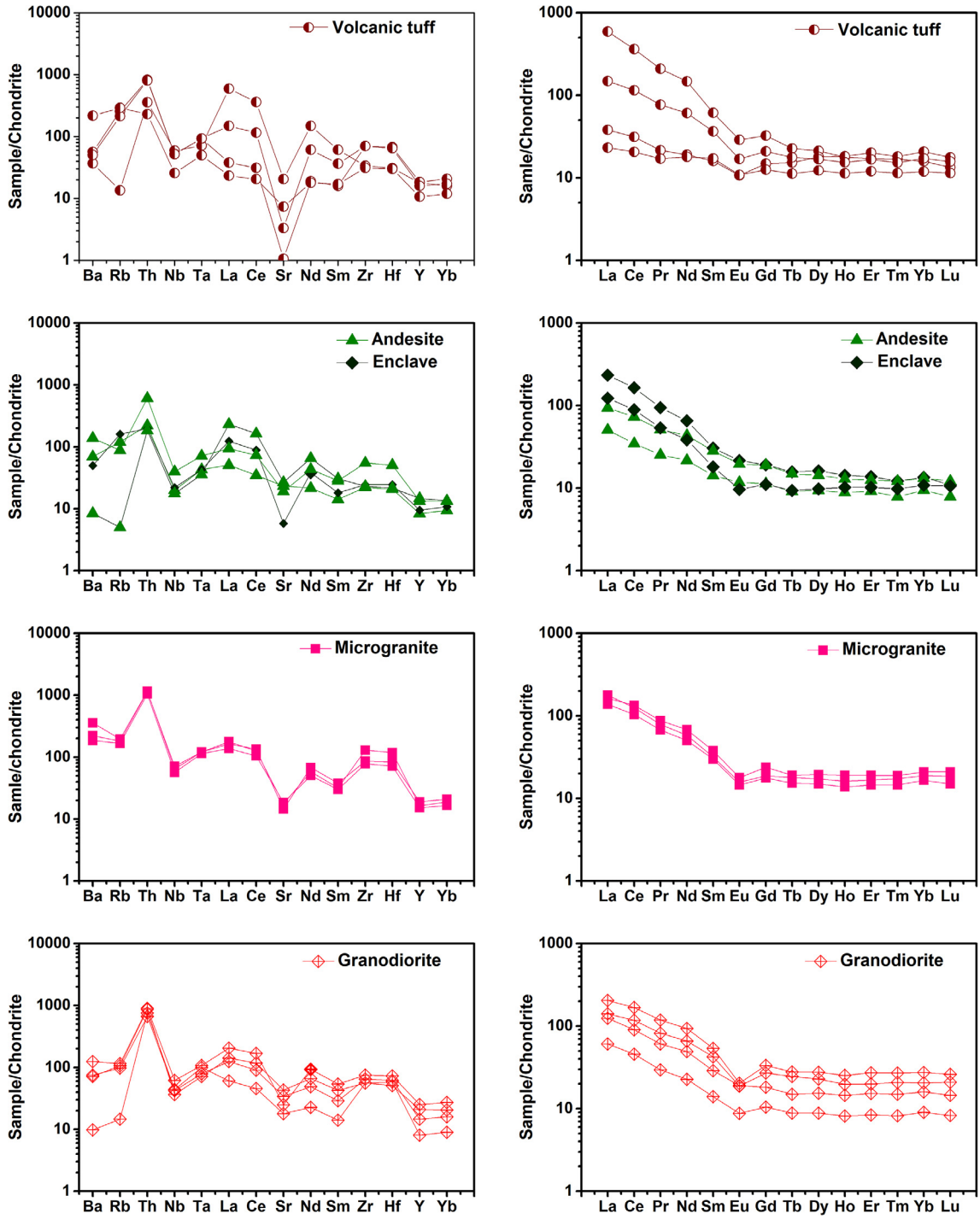

Fig. 12. Chondrite–normalised trace element and REE of the Oued Amizour granitoids.

et al., 2007). The sulphur isotopic composition of the Oued Amisour sulphates (+13.2 to +20.6‰) is much closer to that of coeval Miocene seawater suphates ($\delta^{34}S \approx +22‰$; e.g., Cendón et al., 2004; Hryniv et al., 2007) than that of igneous sulphur ($\delta^{34}S \approx -3$ to +3‰). The data indicate that the sulphate sulphur originates directly from Miocene seawater sulphate, though a mixture with low $\delta^{34}S$ sulphate sulphur derived from disproportionation of magmatic-hydrothermal fluid is not excluded, especially proximal to the Zn-mineralised zone. This is shown in the $\delta^{34}S$ values of anhydrite and gypsum of +13.2 and +14.7‰, respectively, at the top of the anhydrite layer close to the main Zn ore, and +20.6 and +19.3‰ at the bottom, in the anhydrite-gypsum veins within the granodiorites. Mixing between seawater and hydrothermal solution is already alluded by Ogawa et al. (2007) when studying the mechanisms for anhydrite and gypsum formation in the Kuroko massive sulfide-sulfate deposits, north Japan.

The calculation of the oxygen isotope composition of the hydrothermal fluid in equilibrium with the analysed gangue carbonate samples is carried out in order to determine the origin the mineralising fluid (s). The fluid inclusion microthermometric investigation performed on anhydrite and calcite samples gave homogenisation temperatures (Th) range from 170 to 202 °C, with a maximum frequency at 190 °C for anhydrite and 220 to 224 °C with a peak at 222 °C for the gangue calcite. The salinities vary between 22.3 and 26.6 wt% eq. NaCl for anhydrite and from 22.3 to 23.0 wt% eq. NaCl for calcite (see above).

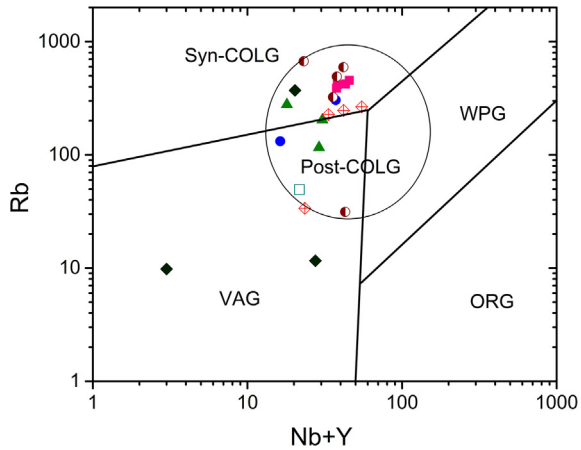

Fig. 13. (Y + Nb) versus Rb (Pearce et al., 1984) diagram to distinguish the tectonic setting of the Oued Amizour magmatic rocks; the area showing the post-collisional setting is from Pearce (1996) (sample symbols as in Fig. 10).

These data indicate that the fluid temperature is relatively hot within main sulphide ore body and decreases slightly towards the anhydrite layer, whereas salinity of the fluid increases. The oxygen isotope composition of the fluid in equilibrium with the gangue calcites was calculated for this range of temperature, using the temperature dependent calcite-H_2O fractionation factor of Friedman and O'Neil (1977). The calculated $\delta^{18}O_{fluid}$ cover a range between +2.9‰ and +7.8‰ (mean = +5.3‰; two calcite samples with anomalously low $\delta^{18}O$ are excluded (samples 19ca f: +11.2‰ and 060 ca: +12.7‰)). The high temperatures coupled with ^{18}O-rich ore fluids, relative to seawater and meteoric waters, are consistent with dominant magmatic–hydrothermal fluids. de Ronde (1995) has previously suggested that a magmatic–hydrothermal origin could account for elevated salinities in VHMS-style mineralisation. Moreover, Huston et al. (2011) pointed out that the evidence for magmatic–hydrothermal contributions to VHMS deposits includes extreme enrichment of ore fluids in ^{18}O ($\delta^{18}O$ > 5‰) and consistently elevated ore fluid salinities relative to modern seawater (more than three times). As these two characteristics are difficult to produce from known processes that modify seawater in VHMS systems, they are considered to be strong evidence for the incorporation of magmatic–hydrothermal fluids. Other evidence for magmatic–hydrothermal contributions to the Oued Amizour Zn deposit is the occurrence of aluminous advanced argillic alteration assemblages (e.g., kaolinite, pyrophyllite, montmorillonite and illite (see above)). The occurrence of such advanced argillic alteration in some VHMS deposits where magmatic-hydrothermal fluids played a major role in the ore deposition is reported by Sillitoe et al. (1996); Huston and Kamprad (2001); Dubé et al. (2007). This alteration process is interpreted to have been caused by disproportionation of SO_2 in

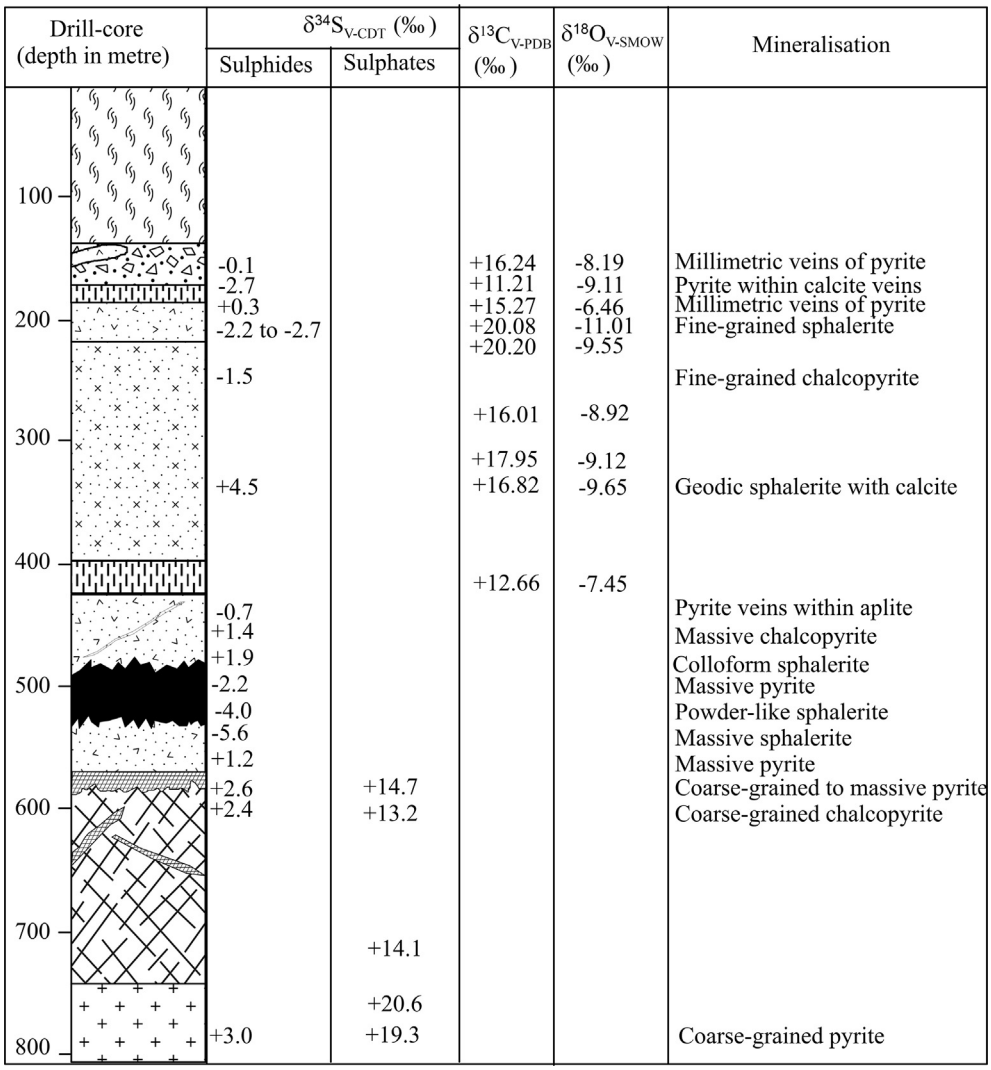

Fig. 14. Distribution of the stable S, O and C isotope data through the whole igneous suite.

magmatic–hydrothermal fluids derived from oxidised magmas in these VHMS deposits (Huston et al., 2011 and references therein).

The same gangue calcite samples analysed for oxygen isotopes also provided carbon isotope ratios. Their carbon isotopic composition is depleted in ^{13}C, with values ranging from −3.7 to −11‰ (see Table 4). Similar to many VHMS (Huston, 1999), there is no correlation between $\delta^{13}C$ and $\delta^{18}O$ (r = 0.03). The observed $\delta^{13}C$ values of calcite samples could have been derived (i) by mixing seawater carbonate with carbon derived from oxidation of methane produced by degradation of organic carbon ($\delta^{13}C$ values of –20 to –30‰: Berger and Vincent, 1986) in underlying sedimentary rocks as suggested for some VHMS deposits (Huston, 1999), (ii) by mixing of seawater carbonate with carbon of igneous derivation ($\delta^{13}C$ values of –5 to –10‰: Ohmoto and Goldhaber, 1997) or (iii) through thermal processing of organic matter, with oxygen supplied from water. Input of marine carbon (with $\delta^{13}C$ values typically ranging from −3 to +3‰) into the mineralising fluid is possibly shown in the two relatively ^{13}C-enriched calcite samples (−3.7 and −4.5‰).

9. Conclusions

The Oued Amizour magmatic complex is composed of igneous rocks with diverse compositions and emplacement style. They vary from plutonic (granodiorites) through sub-volcanic (microgranites) to volcanic rocks (pyroclastites, andesites, lava flows). These rocks exhibit a calc-alkaline character and are mainly highly potassic to shoshonitic. Petrological and geochemical data as well as geotectonic discrimination diagrams indicate that the Oued Amizour magmatic rocks are post-collisional I-type, the Kabylian subcontinental lithospheric mantle previously metasomatised during the Paleogene subduction of the Tethys oceanic lithosphere being the most likely source of the magmas. The emplacement of these granitoids was accompanied by hydrothermal fluids responsible for the deposition of the largest Zn-deposit (sphalerite with minor base metal sulphides, such as pyrite, galena and chalcopyrite) in Algeria. Stable S, O, and C isotopic composition of the sulphides, sulphates and gangue calcite indicate: (1) a major contribution of a relatively hot (~200 °C) and saline (between 22.3 and 26.6% eq. NaCl) magmatic fluid to the generation of primary sulphide mineralisation: (2) the contribution of Miocene seawater sulphur for the generation of anhydrite; and (3) the input of organic carbon from unconsolidated mudstone and/or magmatic carbon (with negative $\delta^{13}C$ values) into the fluids during the calcitisation processes. The detailed metallogenetic and isotopic studies of the deposit as well as the different alteration processes indicate that the mineralisation is part of the VHMS group with a Kuroko-type signature.

Acknowledgments

The authors wish to thank WMZ (Western Mediterranean Zinc) and Terramin Australia companies for providing access to field and sampling bore-holes at the conservation store. They are also grateful to T. Donnelly, A. Tait and J. Dougans for isotope analyses technical support. Adrian J. Boyce is funded by NERC support of the Isotope Community Support Facility at SUERC. Abdelmalek Lekoui wishes to thank the University of Jijel for providing several short period grants to Tunisia.

Appendix A. Supplementary data

Supplementary data associated with this article can be found, in the online version, at https://doi.org/10.1016/j.oregeorev.2018.07.026.

References

Abbassene, F., Chazot, G., Bellon, H., Bruguier, O., Ouabadi, A., Maury, R.C., Déverchère, J., Bosch, D., Monié, P., 2016. A 17 Ma onset for the post-collisional K-rich calc-alkaline magmatism in the Maghrebides: evidence from Bougaroun (northeastern Algeria) and geodynamic implications. Tectonophysics 674, 114–134.
Ahmed-Said, Y., Leake, B.E., Rogers, G., 1993. The petrology, geochemistry and petrogenesis of the Edough igneous rocks, Annaba, NE Algeria. J. Afr. Earth Sci. 17, 1–13.
Arribas, A. Jr., 1995. Characteristics of high-sulfidation epithermal deposits, and their relation to magmatic fluid. In: Thomson, J.F.H. (Ed.), Magmas, Fluids, and Ore Deposit. Mineralogical Association of Canada Short Course Series 23, pp. 419–454.
Auzende, J.-M., Bonnin, J., Olivet, J.-L., 1975. La marge nord-africaine considérée comme marge active. Bull. Soc. Géol. France 7, 486–495.
Bellon, H., 1976. Séries magmatiques néogènes et quaternaires du pourtour méditerranéen occidental, comparées dans leur cadre géochronométriques. Implications géodynamiques. Université Paris-Sud-Orsay, pp. 367 Thèse d'État.
Bellon, H., 1981. Chronologie radiométrique K-Ar des manifestations magmatiques autour de la Méditerranée occidentale entre 33 et 1 Ma. In: Wezel, F.C. (Ed.), Sedimentary Basins of Mediterranean Margins. Technoprint, Bologne, pp. 341–360.
Benali, H., 2007. Les minéralisations associées aux roches magmatiques tertiaires du Nord de l'Algérie: Typologie, pétrologie, cadre géodynamique et implications métallogéniques. Doct. thesis. USTHB, Algiers, pp. 195.
Berger, W.H., Vincent, E., 1986. Deep sea carbonates: reading the carbon isotope signal. Geol. Rundschau 75, 249–269.
Bodnar, R.J., Bethke, P.M., 1984. Systematics of stretching of fluid inclusions, I: fluorite and sphalerite at 1 atmosphere confining pressure. Econ. Geol. 79, 141–161.
Borisenski, A.S., 1977. Cryogenic technique applied to studies of the saline composition of solution in gaseous fluid inclusion in mineral. Akadem. Nauk. CCCP 8, 16–21.
Bossière, G., Peucat, J.J., 1985. New geochronological information by Rb-Sr and U-Pb investigations from the pre-Alpine basement of Grande-Kabylie (Algérie). Can. J. Earth Sci. 22, 675–685.
Bouabsa, L., Marignac, C., Chabbi, R., Cuney, M., 2010. The Filfila (NE Algeria) topaz-bearing granites and their rare metal minerals: Petrologic and metallogenic implications. J. Afr. Earth Sci. 56, 107–113.
Carminati, E., Lustrino, M., Doglioni, C., 2012. Geodynamic evolution of the central and western Mediterranean: tectonics vs. igneous petrology constraints. Tectonophysics 579, 173–192.
Cendón, D.I., Peryt, T.M., Ayora, C., Pueyo, J.J., Taberner, C., 2004. The importance of recycling processes in the Middle Miocene Badenian evaporite basin (Carpathian foredeep): palaeoenvironmental implications. Palaeogeogr. Palaeoclimatol. Palaeoecol. 212, 141–158.
Chappell, B.W., White, A.J.R., 1974. Two contrasting granite types. Pac. Geol. 8, 173–174.
Chappell, B.W., White, A.J.R., 2001. Two contrasting granite types – 25 years later. Aust. J. Earth Sci. 48, 489–499.
Chazot, G., Abbassene, F., Maury, R.C., Déverchère, J., Bellon, H., Ouabadi, A., Bosch, D., 2017. An overview on the origin of post-collisional Miocene magmatism in the Kabylies (northern Algeria): evidence for crustal stacking, delamination and slab detachment. J. Afr. Earth Sci. 125, 27–41.
Chi, G., Ni, P., 2007. Equations for calculation of NaCl/(NaCl + $CaCl_2$) ratios and salinities from hydrohalite-melting and ice-melting temperatures in H_2O-NaCl-$CaCl_2$ system. Acta Petrol. Sin. 23, 33–37.
Chiba, H., Uchiyama, N., Teagle, D.A.H., 1998. Stable isotope study of anhydrite and sulfide minerals at the TAG hydrothermal mound, Mid-Atlantic Ridge, 26°N. Proc. Ocean Drill Prog. Sci. Results 158, 85–90.
Cohen, C.R., 1980. Plate tectonic model for the Oligo-Miocene evolution of the western Mediterranean. Tectonophysics 68, 283–331.
Cook, N.J., Hoefs, J., 1997. Sulphur isotope characteristics of metamorphosed Cu-(Zn) volcanogenic massive sulphide deposits in the Norwegian Caledonides. Chem. Geol. 135, 307–324.
Craig, H., 1957. Isotopic standards for carbon and oxygen and correction factors for mass-spectrometric analysis of carbon dioxide. Geochim. Cosmochim. Acta 12, 133–149.
Craig, H., 1965. Measurement of oxygen isotope paleotemperatures. In: Tongiorgi, E. (Ed.), Stable Isotopes in Oceanographic Studies and Paleotemperatures. CNR Lab. Geol. Nucl, Pisa, pp. 161–182.
Crawford, M.L., 1981. Phase equilibria in aqueous fluid inclusions. Mineral. Assoc. Can. Short Course Handb. 6, 75–100.
Culbert, R., 1972. Abnormalities in the distribution of K, Rb, and Sr in the Coast Mountain batholith. Br. Columbia: Geochim. Cosmochim. Acta 36, 1091–1100.
de Ronde, C.E.J., 1995. Fluid chemistry and isotope characteristics of seafloor hydrothermal systems and associated VMS deposits: potential for magmatic contributions. Miner. Assoc. Can. Short Course Ser. 23, 479–509.
Dubé, B., Mercier-Langevin, P., Hannington, M.D., Gosselin, G., Gosselin, P., 2007. The La Ronde Penna world-class Au-rich volcanogenic massive sulphide deposit, Abitibi, Quebéc: mineralogy and geochemistry of alteration and implications for genesis and exploration. Econ. Geol. 102, 633–666.
Durand-Delga, M., 1978. Alpine chains of the western Mediterranean (Betic Cordilleras and Maghrebides). In: Lemoine, M. (Ed.), Geological Atlas of Alpine Europe and Adjoining Alpine Areas. Elsevier, Amsterdam, pp. 163–225.
Durand-Delga, M., Fontboté, J.-M., 1980. Le cadre structural de la Méditerranée occidentale. 26th Int. Geol. Congress, Paris, Geology of the Alpine chains born of the Tethys. Mém. BRGM 115, 67–85.
Farrell, C.L., Holland, H.D., 1983. Strontium isotope geochemistry of the Kuroko deposits. Econ. Geol. Monograph 5, 302–319.
Fougnot, J., 1990. Le magmatisme miocène du littoral nord constantinois. Doct. Thesis. INPL, Nancy, France, pp. 358.
Fourcade, S., Capdevila, R., Ouabadi, A., Martineau, F., 2001. The origin and geodynamic significance of the Alpine cordierite-bearing granitoids of northern Algeria. a combined petrological, mineralogical, geochemical and isotopic (O, H, Sr, Nd) study. Lithos 57, 187–216.
Franklin, J.M., Lydon, J.W., Sangster, D.F., 1981. Volcanic associated massive sulfide

deposits. Econ. Geol. 75th Anniv. Vol, 485–627.
Friedman, I., O'Neil, J.R., 1977. Compilation of stable isotope fractionation factors of geochemical interest. U.S. Geol. Surv. Prof. Paper 440-kk, 12.
Gemmell, J.B., Fulton, R., 2001. Geology, genesis and exploration implications of the footwall and hanging-wall alteration associated with the Hellyer volcanic-hosted massive sulphide deposit, Tasmania, Australia. Econ. Geol. 96, 1003–1035.
Gemmell, J.B., Large, R.R., 1992. Stringer system and alteration zones underlying the Hellyer volcanogenic massive sulfide deposit, Tasmania, Australia. Econ. Geol. 87, 620–649.
Graine, K., Marignac, C., 2001. Dépôts pyriteux et minéralisations Zn-Pb-(Cu) du massif volcano- plutonique d'Amizour (Bejaïa, Algérie). typologie et genèse des minéralisations. Bull. Serv. Géol. Algérie 11 (1), 97–127.
Gravelle, M., 1959. Études géologiques et prospection minière dans le massif d'Oued Amizour (Algérie). Bull. Serv. Carte Géol. Algérie 28, 149–216.
Hilly, J., 1962. Etude géologique du massif de l'Edough et du Cap de Fer (Est-Constantinois). Pub. Serv. Carte Géol. Algérie (Nlles séries) 19, 408.
Hryniv, S., Parafiniuk, J., Peryt, T.M., 2007. Sulphur isotopic composition of K-Mg sulphates of the Miocene evaporites of the Carpathian Foredeep, Ukraine. Geol. Soc. London Spec. Publ. 285, 265–273.
Huston, D.L., 1999. Stable isotopes and their significance for understanding the genesis of volcanic-hosted massive sulfide deposits: a review. Rev. Econ. Geol. 10, 151–180.
Huston, D.L., Kamprad, J., 2001. Zonation of alteration facies at Western Tharsis: implications for the genesis of Cu–Au deposits, Mount Lyell field, western Tasmania. Econ. Geol. 96, 1123–1132.
Huston, D., Relvas, J.M.R.S., Gemmell, B., Drieberg, S., 2011. The role of granites in volcanic-hosted massive sulphide ore-forming systems: an assessment of magmatic-hydrothermal contributions to the ores. Miner. Deposita 46, 473–508.
Irvine, T.N., Baragar, W.R.A., 1971. A guide to the chemical classification of the common volcanic rocks. Can. J. Earth Sci. 8, 523–548.
Lambert, I.B., Sato, T., 1974. The Kuroko and associated ore deposits of Japan: a review of their features and metallogenesis. Econ. Geol. 69, 1215–1236.
Laouar, R., Boyce, A.J., Ahmed-Said, Y., Ouabadi, A., Fallick, A.E., Toubal, A., 2002. Stable isotope study of the igneous, metamorphic and mineralized rocks of the Edough complex, Annaba, northeast Algeria. J. Afr. Earth Sci. 35, 271–283.
Laouar, R., Boyce, A.J., Arafa, M., Ouabadi, A., Fallick, A.E., 2005. Petrological, geochemical, and stable isotope constraints on the genesis of the Miocene igneous rocks of Chetaibi and Cap de Fer (NE Algeria). J. Afr. Earth Sci. 41, 445–465.
Le Bel, L., Oudin, E., 1982. Fluid inclusion studies of deep-sea hydrothermal sulphide deposits on the East Pacific Rise near 21°N. Chem. Geol. 37, 129–136.
Le Maitre, R.W. (Ed.), 2002. Igneous Rocks. A Classification and Glossary of Terms. Recommendations of the International Union of Geological Sciences Subcommission on the Systematics of Igneous Rocks, second ed. Cambridge University Press, pp. 236.
Leikine, M., 1974. Essai d'interprétation structurale d'une transversale au SW de Bejaia (Algérie): Les Babors et la région subbaborienne. Bull. Soc. Hist. Nat. Afrique Nord 65, 439–459.
Leikine, M., 1971. Etude géologique des Babors occidentaux. Doct. Etat thesis. Univ. Paris, pp. 536.
Marignac, C., Zimmermann, J.L., 1983. Ages K/Ar de l'événement hydrothermal et des intrusions associées dans le district minéralisé miocène d'Aïn-Barbar (Est Constantinois, Algérie). Miner. Deposita 18, 457–467.
Marignac, C., 1983. The Polymetallic Ore Veins of Aïn-Barbar (Algeria) as a Consequence of Alpine Geothermal Activity. In: Schneider, H.J. (Ed.), Mineral Deposits of the Alps and of the Alpine Epoch in Europe. Special Publication No. 3 of the Society for Geology Applied to Mineral Deposits. Springer, Berlin, Heidelberg, pp. 298–312.
Matsubaya, O., Sakai, H., 1973. Oxygen and hydrogen isotopic study on the water of crystallization of gypsum from the Kuroko type mineralization. Geochem. J. 7, 153–165.
Maury, R.C., Fourcade, S., Coulon, C., El Azzouzi, M., Bellon, H., Ouabadi, A., Semroud, B., Megartsi, M., Cotten, J., Belanteur, O., Louni-Hacini, A., Coutelle, A., Piqué, A., Capdevila, R., Hernandez, J., 2000. Post-collisional Neogene magmatism of the Mediterranean Maghreb margin: a consequence of slab detachment. C.R. Acad. Sci. Paris 331, 159–173.
McCrea, J.M., 1950. On the isotopic chemistry of carbonates and paleotemperature scale. J. Chem. Phys. 18, 849–857.
Monié, P., Maluski, H., Saadallah, A., Caby, R., 1988. New ^{39}Ar-^{40}Ar ages of Hercynian and Alpine thermotectonic events in Grande Kabylie (Algeria). Tectonophysics 152, 53–69.
Obert, D., 1981. Géologie des Babors (Algérie): importance de la paléotectonique alpine dans l'orogenèse alpine. Rev. Geol. Dyn. Géogr. Phys. 25 (2), 99–117.
Ogawa, Y., Shikazono, N., Ishiyama, D., Sato, H., Mizuta, T., Nakano, T., 2007. Mechanisms for anhydrite and gypsum formation in the Kuroko massive sulfide-sulfate deposits, north Japan. Miner. Deposita 42, 219–233.
Ohmoto, H., 1996. Formation of volcanogenic massive sulfide deposits: The Kuroko perspective. Ore Geol. Rev. 10, 135–177.
Ohmoto, H., Goldhaber, M.B., 1997. Sulfur and carbon isotopes. In: Barnes, H.L. (Ed.), Geochemistry of Hydrothermal Ore Deposits, third ed. Wiley, New York, pp. 517–611.
Ohmoto, H., Rye, D., 1979. Isotopes of sulfur and carbon. In: Barnes, H.L. (Ed.), Geochemistry of Hydrothermal Ore Deposits, 2nd ed. Wiley, New York, pp. 509–567.
Ohmoto, H., Drummond, S.E., Eldridge, C.S., Pisutha-Arnond, V., Lenagh, T.C., 1983. Chemical processes of ore formation. Econ. Geol. Monogr. 5, 570–604.
Ohmoto, H., 1986. Stable isotope geochemistry of ore deposits. In: Valley, J.W., Taylor, H. P. Jr., O'Neil J.R. (Eds.), Stable Isotopes in High Temperature Geological Processes. Reviews in Mineralogy Vol. 16, Mineral. Soc. Am. pp. 491–560.
Ouabadi, A., Capdevila, R., Fourcade, S., Semroud, B., 1992. Le granite à biotite et cordiérite du Cap Bougaroun (Algérie): un analogue alpin des granites de type S de la ceinture de Lachlan (Australie)? C.R. Acad. Sci. Paris 314, 1187–1194.
Ouabadi, A., 1994. Pétrologie, géochimie et origine des granitoïdes peralumineux à cordiérite (Cap Bougaroun, Béni-Touffout et Filfila), Algérie nord-orientale. Doct. thesis. Univ. Rennes I, France, pp. 257.
Paytan, A., Kastner, M., Campbell, D., Thiemens, M.H., 1998. Sulfur isotopic composition of Cenozoic seawater sulfate. Science 282, 1459–1462.
Pearce, J.A., 1996. Source and setting of granitic rocks. Episodes 19, 120–125.
Pearce, J.A., Harris, N.B.W., Tindle, A.G., 1984. Trace element discrimination diagrams for the tectonic interpretation of granitic rocks. J. Petrol. 25, 956–983.
Peccerillo, A., Taylor, S.R., 1976. Geochemistry of Eocene calc-alkaline volcanic rocks from the Kastamonu area, northern Turkey. Contr. Mineral. Petrol. 58, 63–81.
Robinson, B.W., Kusakabe, M., 1975. Quantitative preparation of sulfur dioxide, for $^{34}S/^{32}S$ analyses, from sulfides by combustion with cuprous oxide. Anal. Chem. 47, 1179–1181.
Roedder, E., 1984b. The fluids in salt. Am. Mineral. 69, 413–439.
Roedder, E., 1984. Fluid Inclusions. In: Reviews in Mineralogy; Mineralog. Soc. America, vol. 12, p. 604.
Sakai, H., Des Marais, D.J., Ueda, A., Moore, J.G., 1984. Concentrations and isotope ratios of carbon, nitrogen and sulfur in ocean-floor basalts and volcanic gases at Kilauea volcano, Hawaii. Geochim. Cosmochim. Acta 48, 2433–2441.
Sasaki, A., 1970. Seawater sulfate as a possible determinant for sulfur isotopic compositions of some strata-bound sulfide ores. Geochem. J. 4, 41–51.
Semroud, B., Maury, R.C., Ouabadi, A., Cotton, J., Fourcade, S., Fabries, J., Gravelle, M., 1994. Géochimie des granitoides miocènes de Béjaia-Amizour (Algérie du Nord). C.R. Acad. Sci. Paris 318, 95–102.
Semroud, B., 1981. Evolution pétrologique du complexe magmatique Néogène de la région de Béjaia-Amizour. Doct. thesis. USTHB, Algiers, pp. 267.
Sharman, E.R., Taylor, B.E., Minarik, W.G., Dubé, B., Wing, B.A., 2015. Sulfur isotope and trace element data from ore sulfides in the Noranda district (Abitibi, Canada): implications for volcanogenic massive sulfide deposit genesis. Miner. Deposita 50, 591–606.
Shikazono, N., Holland, H.D., Quirk, R.F., 1983. Anhydrite in Kuroko deposits, mode of occurrence and depositional mechanism. Econ. Geol. Monogr. 5, 329–344.
Sillitoe, R.H., Hannington, M.D., Thompson, J.F.H., 1996. High sulfidation deposits in the volcanogenic massive sulfide environment. Econ. Geol. 91, 204–212.
Solomon, M., Eastoe, C.J., Walshe, J.L., Green, G.R., 1988. Mineral deposits and sulfur isotope abundances in the Mount Read Volcanics between Que River and Mount Darwin. Econ. Geol. 83, 1307–1328.
Taylor, S.R., 1965. Application of trace elements data to problems in petrology. Phys. Chem. Earth 6, 133–213.
Taylor, S.R., 1969. Trace element chemistry of andesites and associated calc-alkaline rocks. Oregon Dept. Geol. Mineral Ind. Bull. 65, 43–63.
Taylor, B.E., 1987. Stable isotope geochemistry of ore-forming fluids. Mineral. Assoc. Can. Short Course Ser. 13, 337–445.
Teagle, D.A.H., Alt, J.C., Chiba, H., Humphris, S.E., Halliday, A.N., 1998. Strontium and oxygen isotopic constraints on fluid mixing, alteration and mineralization in the TAG hydrothermal deposits. Chem. Geol. 149, 1–24.
Torró, L., Proenza, J.A., Melgarejo, J.C., Alfonso, P., Farré de Pablo, J., Colomer, J.M., García-Casco, A., Gubern, A., Gallardo, E., Cazañas, X., Chávez, C., Del Carpio, R., León, P., Nelson, C.E., Lewis, J.F., 2016. Mineralogy, geochemistry and sulfur isotope characterization of Cerro de Maimón (Dominican Republic), San Fernando and Antonio (Cuba) lower Cretaceous VMS deposits: Formation during subduction initiation of the proto-Caribbean lithosphere within a fore-arc. Ore Geol. Rev. 72, 794–817.
Vila, J.M., 1980. La chaîne alpine d'Algérie orientale et des confins algéro-tunisiens. Doct. Etat thesis. Univ. Paris VI, pp. 663.
Villemaire, Cl, 1987. Les amas sulfurés du massif miocène d'El Aouana (Algérie). Dynamisme de mise en place des roches volcaniques et implications métallogéniques. J. Afr. Earth Sci. 7, 133–148.
Wilson, M., 2007. In: Igneous Petrogenesis. Springer, pp. 480.
Yeats, C.J., Hollis, S.P., Halfpenny, A., Corona, J.-C., LaFlamme, C., Southam, G., Fiorentini, M., Herrington, R.J., Spratt, J., 2017. Actively forming Kuroko-type volcanic-hosted massive sulfide (VHMS) mineralization at Iheya North, Okinawa Trough. Ore Geol. Rev. 84, 20–41.